JOURNAL OF BACTERIOLOGY, June 2004, p. 4000–4013 Vol. 186, No. 12
0021-9193/04/$08.00+0 DOI: 10.1128/JB.186.12.4000–4013.2004

Role of the Anti-Sigma Factor SpoIIAB in Regulation of σ^G during *Bacillus subtilis* Sporulation

Mónica Serrano,[1] Alexandre Neves,[1]† Cláudio M. Soares,[1] Charles P. Moran, Jr.,[2] and Adriano O. Henriques[1]*

Instituto de Tecnologia Química e Biológica, Universidade Nova de Lisboa, 2781-901 Oeiras Codex, Portugal,[1] and Department of Microbiology, Emory University School of Medicine, Atlanta, Georgia 30322[2]

Received 27 October 2003/Accepted 16 February 2004

RNA polymerase sigma factor σ^F initiates the prespore-specific program of gene expression during *Bacillus subtilis* sporulation. σ^F governs transcription of *spoIIIG*, encoding the late prespore-specific regulator σ^G. However, transcription of *spoIIIG* is delayed relative to other genes under the control of σ^F, and after synthesis, σ^G is initially kept in an inactive form. Activation of σ^G requires the complete engulfment of the prespore by the mother cell and expression of the *spoIIIA* and *spoIIIJ* loci. We screened for random mutations in *spoIIIG* that bypassed the requirement for *spoIIIA* for the activation of σ^G. We found a mutation (*spoIIIGE156K*) that resulted in an amino acid substitution at position 156, which is adjacent to the position of a mutation (E155K) previously shown to prevent interaction of SpoIIAB with σ^G. Comparative modelling techniques and in vivo studies suggested that the *spoIIIGE156K* mutation interferes with the interaction of SpoIIAB with σ^G. The σ^{GE156K} isoform restored σ^G-directed gene expression to *spoIIIA* mutant cells. However, expression of *sspE-lacZ* in the *spoIIIA spoIIIGE156K* double mutant was delayed relative to completion of the engulfment process and was not confined to the prespore. Rather, β-galactosidase accumulated throughout the entire cell at late times in development. This suggests that the activity of σ^{GE156K} is still regulated in the prespore of a *spoIIIA* mutant, but not by SpoIIAB. In agreement with this suggestion, we also found that expression of *spoIIIGE156K* from the promoter for the early prespore-specific gene *spoIIQ* still resulted in *sspE-lacZ* induction at the normal time during sporulation, coincidently with completion of the engulfment process. In contrast, transcription of *spoIIIGE156K*, but not of the wild-type *spoIIIG* gene, from the mother cell-specific *spoIID* promoter permitted the rapid induction of *sspE-lacZ* expression. Together, the results suggest that SpoIIAB is either redundant or has no role in the regulation of σ^G in the prespore.

Gene expression in the prespore and mother cell chambers of sporulating *Bacillus subtilis* is controlled by RNA polymerase sigma subunits whose activity is restricted to a specific cell type (22, 31, 37, 46). The activation of the sporulation-specific sigma factors is tightly coupled to the completion of key morphological intermediates in the process and also relies on signaling pathways that operate between the two cell types and that keep the prespore and mother cell lines of gene expression in close register (22, 31, 37, 46). Soon after the asymmetric division of the sporangial cell, an event that creates the prespore and the much larger mother cell, the first compartment-specific sigma factor σ^F becomes active in the prespore (22, 31, 37, 46). σ^F triggers the activation of σ^E in the mother cell, which together with σ^F drive the migration of the septal membranes around the prespore. This process is termed engulfment and results in the formation of a protoplast isolated from the external medium, fully encircled by the mother cell cytoplasm (22, 31, 37, 46). After engulfment, σ^F is replaced by σ^G, which controls late stages of development in this compartment and which also triggers the activation of the late mother cell-specific regulator σ^K (22, 31, 37, 46). The activities of both σ^G and σ^K are required for the assembly of the protective layers that encase the mature spore (22, 31, 37, 46).

Synthesis of σ^F occurs in the predivisional cell, but its activation is restricted to the prespore by the action of three regulatory proteins, SpoIIAA, SpoIIAB, and SpoIIE. SpoIIAB is an anti-sigma factor that binds to σ^F as a dimer, preventing its association with RNA polymerase, whereas SpoIIAA is an anti-anti-sigma factor that in an unphosphorylated state interacts with SpoIIAB and releases σ^F from the SpoIIAB-σ^F complex (1, 2; reviewed in references 31 and 37). SpoIIE is a septum-bound phosphatase that is also produced in the predivisional cell that promotes the preferential dephosphorylation of SpoIIAA-P in the prespore (reviewed in references 31 and 37).

The transcriptional activity of σ^F can be divided into an early phase and a late phase. Transcription of the *spoIIIG* gene (encoding σ^G) is induced as part of the late phase, towards the end of the engulfment process (29). After synthesis, σ^G does not become active until the engulfment process is complete (29). Once activated and since σ^G efficiently recognizes its own promoter, its cellular levels increase rapidly, allowing for the deployment of the σ^G regulon (17, 47). Because of this autoregulation, both the late transcription of *spoIIIG* and the negative regulation of σ^G appear to ensure that its transcriptional activity is effectively coupled to completion of the engulfment process and does not occur prematurely or ectopically (31, 37, 45). The tight coupling of σ^G activation to the conclusion of the engulfment sequence may serve to ensure that biogenesis of

* Corresponding author. Mailing address: Instituto de Tecnologia Química e Biológica, Universidade Nova de Lisboa, Avenida da República, Apartado 127, 2781-901 Oeiras Codex, Portugal. Phone: 351-21-4469521. Fax: 351-21-4411277. E-mail: aoh@itqb.unl.pt.

† Present address: Fred Hutchinson Cancer Research Center, Seattle, WA 98109.

the spore integuments is not initiated during movement of the engulfment membranes (31, 37, 45, 46).

Conclusion of the engulfment process is not sufficient for the activation of σ^G, which further requires expression of several genes, including the eight cistrons of the *spoIIIA* operon and the *spoIIIJ* gene (6, 19, 34). σ^G accumulates in *spoIIIA* or *spoIIIJ* mutant cells but is unable to activate transcription from its target promoters (19, 41). The *spoIIIA* operon encodes several putative membrane proteins and is expressed in the mother cell under the direction of σ^E (15). The *spoIIIJ* gene is expressed during vegetative growth and encodes a membrane protein translocase of the YidC/Oxap1 family (6, 27, 48). Despite the fact that its product may accumulate in both the prespore and the mother cell (6, 27), expression of *spoIIIJ* in the prespore is sufficient for the activation of σ^G and sporulation (41).

Two negative regulators of σ^G are known, the anti-sigma factor SpoIIAB and the LonA protease (3, 8, 19, 21, 35, 40). Expression of *spoIIIG* prior to the asymmetric division of the sporangial cell blocks sporulation, a phenotype that can be suppressed by a multicopy allele of *spoIIAB* (21), and certain point mutations in *spoIIAB* result in expression of σ^G-dependent genes under conditions that do not support efficient sporulation (8, 35). Moreover, SpoIIAB binds to σ^G in vitro under conditions that also promote binding of SpoIIAB to σ^F (19), and the structure of a dimer of *Bacillus stearothermophilus* SpoIIAB in complex with σ^F shows that most of the residues involved in the interaction are conserved in σ^G, but not in other sigma factors (2).

While it seems clear that SpoIIAB can regulate σ^G under nonsporulation conditions or in the predivisional cell at the onset of sporulation, the evidence for a role in the control of σ^G in the prespore is less clear (3, 8, 19, 21, 35). On the one hand, SpoIIAB seems to disappear from the prespore coincidently with the first manifestations of σ^G activity, but it persists in the prespore of a *spoIIIA* mutant (21). In addition, production of a form of σ^G (σ^{GE155K}) that is not efficiently bound by SpoIIAB in vitro allows expression of the σ^G-controlled *sspE* gene in *spoIIIA* or *spoIIIJ* mutants, suggesting that the expression of both loci is required to antagonize the inhibitory action of SpoIIAB upon σ^G (19, 41). However, expression of *sspE* in *spoIIIGE155K* cells bearing mutations in either *spoIIIA* or *spoIIIJ* does not occur prematurely, suggesting that the activity of σ^{GE155K} is still regulated in the double mutants (19, 41). Also, there seems to be very little, if any, free SpoIIAB in the prespore (28), and the anti-sigma factor would have to be able to negatively regulate σ^G at a time when SpoIIAB itself is antagonized by the anti-anti-sigma SpoIIAA in order to release active σ^F (reviewed in references 31 and 37). Since the interaction of SpoIIAB with σ^G appears to be very similar to the interaction of SpoIIAB with σ^F (7), it seems unlikely that at least prior to completion of the engulfment process, SpoIIAB decisively contributes to the regulation of σ^G. Mutations in *lonA*, coding for the ATP-dependent LonA protease, also result in σ^G activity under nonsporulation conditions, and result in some expression of *sspE-lacZ* in cells of a *spoIIIA* mutant during sporulation (40).

Here we have analyzed the role SpoIIAB plays in the regulation of σ^G in sporulating cells. We screened for mutations in *spoIIIG* that allowed expression of the σ^G-controlled *sspE-lacZ* fusion in a *spoIIIA* background and found a single mutation that converted a glutamate at position 156 of σ^G to a lysine. However, we found that expression of *sspE-lacZ* in a *spoIIIGE156K spoIIIA* double mutant was delayed relative to the completion of the engulfment process and was not confined to the prespore. Rather, β-galactosidase accumulated throughout the whole cell at late times of sporulation. We also forced the early expression of *spoIIIGE156K* in the prespore from the *spoIIQ* promoter and found no premature induction of *sspE-lacZ* expression. In contrast, expression of *spoIIIGE156K* in the mother cell readily results in *sspE-lacZ* expression. The results suggest that the activity of σ^G is regulated in the prespore compartment by a SpoIIAB-independent mechanism and that SpoIIAB is either redundant or plays only a minor role.

MATERIALS AND METHODS

Bacterial strains and general methods. The *B. subtilis* strains used in this work (listed in Table 1) are congenic derivatives of the Spo$^+$ strain MB24 (*trpC2 metC3*) (14). Luria-Bertani (LB) medium was used for the maintenance of *Escherichia coli* DH5α (Bethesda Research Laboratories) and *B. subtilis*. Sporulation was induced in Difco sporulation medium (DSM) and assessed as described previously (13). All other general methods were performed as described previously (13).

Structure of a complex between *B. subtilis* SpoIIAB and σ^G by comparative modelling techniques. The structure of the SpoIIAB-σ^F complex from *B. stearothermophilus* (Protein Data Bank code 1LO0) (2) was used here to derive, by comparative modelling techniques, the SpoIIAB-σ^F and SpoIIAB-σ^G complexes from *B. subtilis* (25, 39). The structure of the SpoIIAB-σ^F complex from *B. stearothermophilus* (Protein Data Bank code 1LO0) (2) was used here to derive the SpoIIAB-σ^F and SpoIIAB-σ^G complexes from *B. subtilis*. The structure of SpoIIAB from *B. subtilis* can be modelled on the basis of SpoIIAB from *B. stearothermophilus*, because the two sequences present 75% identity and 90% similarity and only five residues at the C terminus cannot be aligned (25, 39). The structure of the SpoIIAB-σ^F complex from *B. stearothermophilus* contains information for only part of σ^F (from residues 104 to 160), and modelling of the sigma factors was restricted to the residues that are homologous to this segment. For *B. subtilis* σ^F, this segment presents 84% identity and 88% similarity to σ^F from *B. stearothermophilus*, which also suggests that a very good model will be obtained. In contrast, *B. subtilis* σ^G shows 30% identity and 63% similarity with σ^F from *B. stearothermophilus*. The SpoIIAB-σ^F from *B. stearothermophilus* has a bound ADP molecule that was not modelled, because no contacts are made between this region and the sigma factor. Modeller (38) version 6.1 was used for all comparative modelling tasks. Sequences for both proteins in the complex were simultaneously aligned against the X-ray structure of SpoIIAB-σ^F from *B. stearothermophilus*, and 20 models were generated using these alignments. The model showing the lowest value of the objective function was chosen and analyzed using PROCHECK (23). In the case of SpoIIAB-σ^F from *B. subtilis*, the Ramachandran plot showed 87.4% residues in most favored regions, 9.5% residues in additional allowed regions, 2.5% in generously allowed regions, and 0.6% residues in disallowed regions. The residues in disallowed regions, Leu 103 and Arg 105, are homologous to residues in SpoIIAB-σ^F from *B. stearothermophilus* that are also in disallowed regions. This region corresponds to the ADP binding site, and the conformation of these two residues is the most probable one. In the case of SpoIIAB-σ^G from *B. subtilis*, we obtained 88.1% residues in most favored regions, 8.5% residues in additional allowed regions, 3.1% in generously allowed regions, and 0.3% is disallowed regions. In this case, only Arg 105 is in a disallowed zone of the Ramachandran plot, and for the reasons stated above, its conformation was considered the most probable.

Construction of an *sspE-lacZ* fusion. First, a 500-bp HindIII-to-HincII fragment released from pUC12*sspE* (10) was inserted between the SmaI and HindIII sites of pBluescript SKII(+) (Stratagene, La Jolla, Calif.) to generate pAH225. Next, NheI- and EcoRI-digested pAH235 was mixed with the *lacZ* gene released from pPP207 (49) by digestion with SpeI and MscI, and a neomycin resistance (Nm^r) determinant was released from pBEST502 (16) with EcoRI and SmaI. Linearization of the resulting plasmid, pMS53, with ScaI permitted integration of the *sspE-lacZ* fusion into the *sspE* locus of strain MB24, producing strain AH2321 (Table 1). The Δ*sspE*::*sspE-lacZ* allele in strain AH2321 is hereafter abbreviated *sspE-lacZ* for simplicity (Table 1).

Construction of *spoIIIG* mutations. To create an in-frame deletion of the *spoIIIG* gene, a 1.1-kb DNA fragment was first released from pSP72IIIG (19) by digestion with BglII and SalI and inserted between the BglII and XhoI sites of pLitmus 28 (New England Biolabs, Beverly, Mass.) to yield pAH220, which then

TABLE 1. *B. subtilis* strains used in this study

Strain	Relevant genotype[a]	Origin
MB24	*trpC2 metC3*	Laboratory stock (14)
AH62	*trpC2 metC3 spoIIIA*::Tn*917*Ω*HU24*	Laboratory stock (19)
AH1043	*trpC2 metC3* Δ*amyE*::*spoIIIG-gusA*	This work
AH1842	*trpC2 metC3* Δ*amyE*::*spoIIIG*	This work
AH1843	*trpC2 metC3* Δ*spoIIIG*::*cat* Δ*amyE*::*spoIIIG*	This work
AH1870	*trpC2 metC3* Δ*spoIIIG*::*cat*	This work
AH2321	*trpC2 metC3* Δ*sspE*::*sspE-lacZ*	This work
AH2452	*trpC2 metC3* Δ*spoIIIG* Δ*sspE*::*sspE-lacZ*	This work
AH2456	*trpC2 metC3* Δ*spoIIIG* Δ*sspE*::*sspE-lacZ spoIIIA*::Tn*917*Ω*HU24*	This work
AH2460	*trpC2 metC3* Δ*spoIIIG* Δ*sspE*::*sspE-lacZ* Δ*amyE*::P_{spoIID}-*spoIIIG*	This work
AH2461	*trpC2 metC3* Δ*spoIIIG* Δ*sspE*::*sspE-lacZ* Δ*amyE*::P_{spoIID}-*spoIIIGE156K*	This work
AH2462	*trpC2 metC3* Δ*spoIIIG* Δ*sspE*::*sspE-lacZ* Δ*lonA*::*cat*	This work
AH2463	*trpC2 metC3* Δ*spoIIIG* Δ*sspE*::*sspE-lacZ* Δ*lonA*::*cat* Δ*amyE*::P_{spoIID}-*spoIIIG*	This work
AH2464	*trpC2 metC3* Δ*lonA*::*cat*	Laboratory stock (40)
AH2465	*trpC2 metC3* Δ*spoIIIG* Δ*sspE*::*sspE-lacZ* Δ*lonA*::*cat* Δ*amyE*::P_{spoIID}-*spoIIIGE156K*	This work
AH2490	*trpC2 metC3* Δ*spoIIIG* Δ*sspE*::*sspE-lacZ* Δ*amyE*::P_{xylA}-*spoIIIG*	This work
AH2491	*trpC2 metC3* Δ*spoIIIG* Δ*sspE*::*sspE-lacZ* Δ*amyE*::P_{xylA}-*spoIIIGE156K*	This work
AH2492	*trpC2 metC3* Δ*spoIIIG* Δ*sspE*::*sspE-lacZ* Δ*amyE*::P_{xylA}-*spoIIIG* Δ*thrC*::P_{spac}-*spoIIAB*	This work
AH2493	*trpC2 metC3* Δ*spoIIIG* Δ*sspE*::*sspE-lacZ* Δ*amyE*::P_{xylA}-*spoIIIGE156K* Δ*thrC*::P_{spac}-*spoIIAB*	This work
AH3786	*trpC2 metC3* Δ*spoIIIG* Δ*sspE*::*sspE-lacZ* Δ*amyE*::*spoIIIG*	This work
AH3787	*trpC2 metC3* Δ*spoIIIG* Δ*sspE*::*sspE-lacZ* Δ*amyE*::*spoIIIGE156K*	This work
AH3788	*trpC2 metC3* Δ*spoIIIG* Δ*sspE*::*sspE-lacZ* Δ*amyE*::P_{spoIIQ}-*spoIIIG*	This work
AH3789	*trpC2 metC3* Δ*spoIIIG* Δ*sspE*::*sspE-lacZ* Δ*amyE*::P_{spoIIQ}-*spoIIIGE156K*	This work
AH3790	*trpC2 metC3* Δ*spoIIIG* Δ*sspE*::*sspE-lacZ spoIIIA*::Tn*917*Ω*HU24* Δ*amyE*::*spoIIIG*	This work
AH3791	*trpC2 metC3* Δ*spoIIIG* Δ*sspE*::*sspE-lacZ spoIIIA*::Tn*917*Ω*HU24* Δ*amyE*::*spoIIIGE156K*	This work
AH3795	*trpC2* Δ*spoIIIG*	This work
ZB307	Prototrophic	Laboratory stock (52)

[a] For simplicity, the *spoIIIA*::Tn*917*Ω*HU24*, Δ*sspE*::*sspE-lacZ*, Δ*amyE*::P_{spoIID}-*spoIIIG*, Δ*amyE*::P_{spoIID}-*spoIIGE156K*, Δ*amyE*::P_{spoIIQ}-*spoIIIG*, and Δ*amyE*::P_{spoIIQ}-*spoIIIGE156K* alleles are abbreviated *spoIIIA*::Tn*917*, *sspE-lacZ*, P_{spoIID}-*spoIIIG*, P_{spoIID}-*spoIIIGE156K*, P_{spoIIQ}-*spoIIIG*, and P_{spoIIQ}-*spoIIIG*, respectively. Note that the *spoIIIGE156K* allele under the control of its normal promoter or other promoters is always used at the *amyE* locus. Fusions of P_{xylA} to *spoIIIG* alleles at *amyE* or of P_{spac} to *spoIIAB* at *thrC* are abbreviated P_{xylA}-*spoIIIG*, P_{xylA}-*spoIIIGE156K*, or P_{spac}-*spoIIAB*, respectively.

served as a PCR template using primers *spoIIIG*-247R and *spoIIIG*-559D (Table 2). The PCR template was first treated with DpnI and then with PstI and last, it was autoligated, yielding pMS124. Sequencing confirmed the in-frame deletion of codons 13 to 130 of *spoIIIG*. Competent cells of strain MB24 were cotransformed with pMS124 and chromosomal DNA from strain ZB307 (52), with selection for methionine prototrophy. Spo$^-$ congressants appeared at a frequency of about 3%. One, shown by PCR to carry a deletion of the *spoIIIG* gene (referred to as Δ*spoIIIG*) was named AH3795 (Table 1). Strain AH3795 was transformed with ScaI-linearized pMS53 (*sspE-lacZ*) to produce AH2452. Strain AH2452 was then transformed with chromosomal DNA from strain AH62 (*spoIIIA*::Tn*917*ΩHU24, hereafter abbreviated to *spoIIIA*::Tn*917*) (Table 1) to create strain AH2456.

TABLE 2. Primers used in this study

Primer	Sequence (5′→3′)
spoIIIG-247R	TTCATCCTGCAGTCTGCCTAAACAGC
spoIIIG-559D	GGAGCCGACTGCAGAAGACATCGC
spoIIIG-392D	GGGAAAAAAGATCTCGAGAAATAAAGTCG
spec-R	TGTTTGGGAGGATGATTCCACGGTACC
spoIIIG-spoIIQ	GTTGCTGAGGTGATGAAACAGTGTCGAGAA ATAAAGTCG
spoIIIG-spoIID	CGAGCAGGAGGCAGCTGAATGTGTCGAGAA ATAAAGTCG
spoIIIG-761R	CCCGGAGAGATCTTGAGACACGG
spoIIIG-2385R	CCCGGAGTGGATCCTTGAGACACGG
spoIIQ-152D	GTTTCAAAGCTGAATTCCAGGCAGCG
spoIIQ-500R	TGTTTCATCACCTCAGCAACATTCTG
spoIID-1D	CGGAAGAATTCCGCCGTATGAATGG
spoIID-500R	ATTCAGCTGCCTCCTGCTCGGG
P_{xylA}D	GATCAGCGATATCGAATTCATCCACTCC
P_{xylA}R	GTGATTTCCCCCTTAAAAATAAATTC
P_{xylA}-*spoIIIG*	TTTATTTTTAAGGGGGAAATCACGTGTCGAG AAATAAAGTCG
spoIIAB-166D	GAACAGCAGGATCCTGACACTGGGGG
spoIIAB-665R	CCTCCGCATGCATAACAAATCTCC

To create an insertion-deletion *spoIIIG* mutant, a 922-bp DNA fragment containing the *spoIIIG* gene was first released from pSP72IIIG (19) by partial digestion with EcoRI and HindIII and inserted between the EcoRI and HindIII sites of pLitmus 29 (New England Biolabs) to create pMS33. Next, a chloramphenicol resistance (Cm^r) cassette was released from pMS38 (51) by digestion with NsiI and PstI and cloned into PstI-digested pMS33 to yield pMS40. Strain AH1870 (Cm^r) in which disruption of the *spoIIIG* gene by a double-crossover event was verified by PCR resulted from the transformation of strain MB24 with pMS40 (Table 1).

Insertion of an intact copy of the *spoIIIG* gene at *amyE*. A copy of the *spoIIIG* gene was inserted at *amyE* in two steps. We first isolated a 427-bp HindIII-to-BamHI fragment from pTK4 encompassing the *spoIIGB-spoIIIG* intergenic region (20), which was introduced between the HindIII and BamHI sites of the *amyE* integrational vector pMLK83 (18), to create pAH235. Strain AH1043 (AmyE$^-$/Nm^r) (Table 1) resulted from the transformation of strain MB24 with XbaI-linearized pAH235. Then, a spectinomycin resistance (Sp^r) cassette was released from pAH256 (13) by digestion with SpeI and NcoI and cloned between the same sites of pMS33 (see above), yielding pMS37. Last, a fragment carrying the Sp^r determinant and the *spoIIIG* gene was released from pMS37 by digestion with SmaI and EcoRI and cloned between the EcoRI and NruI sites of pDG364 (4). Transformation of AH1043 with the resulting plasmid, pMS45, created AH1842 (Sp^r/Nm^s and Spo$^+$) (Table 1), in which the presence of an intact *spoIIIG* gene at *amyE* was verified by PCR. Transformation of strain AH1842 with chromosomal DNA from AH1870 (Δ*spoIIIG*::*cat*) produced AH1843 (Δ*spoIIIG*::*cat* Δ*amyE*::*spoIIIG* Sp^r) (Table 1).

Random mutagenesis of *spoIIIG*. Strain AH1843 (Table 1) was mutagenized with *N*-methyl-*N*′-nitro-*N*-nitrosoguanidine essentially as described previously (4). The mutagenesis was effective, as 1% of all colonies obtained from the transformation of strain AH1870 (Δ*spoIIIG*::*cat*) (Table 1) with chromosomal DNA from mutagenized AH1843 selecting for Sp^r (which selects for the *spoIIIG* copy at *amyE*) failed to complement the null mutation in the *spoIIIG* gene. In order to select for σ^G mutants that would bypass the need of the *spoIIIA* locus for σ^G activity, chromosomal DNA from mutagenized AH1843 was used to transform AH2456 (Δ*spoIIIG spoIIIA*::Tn*917 sspE-lacZ* [see above]) to Sp^r.

Transformants that showed β-galactosidase activity on DSM plates supplemented with 5-bromo-4-chloro-3-indolyl-β-D-galactopyranoside (X-Gal) (dark blue colonies) were selected and purified. The linkage between the Lac^+ phenotype and the Sp^r marker was verified by retransforming the screening strain AH2456 with chromosomal DNA from the Lac^+ mutants (only mutants showing 100% linkage between the Lac^+ and Sp^r traits or close to 100% linkage were considered). One Lac^+ transformant (AH3791) was selected (Table 1), and the *spoIIIG* gene present at *amyE* was sequenced after PCR amplification using primers *spoIIIG*-392D and *spec*-R. Strain AH3791 was found to harbor a single-nucleotide change (GAA to AAA) at codon 156 of the *spoIIIG* gene. A control strain, AH3790, with the wild-type allele of *spoIIIG* at *amyE*, was constructed by transformation of AH2456 (Δ*spoIIIG spoIIIA*::Tn*917 sspE-lacZ* [see above]) with chromosomal DNA from AH1842. Strains AH3786 and AH3787 were constructed by transformation of AH2452 (Δ*spoIIIG sspE-lacZ* [see above]) with chromosomal DNA from AH1842 and AH3791, respectively.

Fusion of the *xylA* promoter to the *spoIIIG* gene. Initially, the 5′ end of the *spoIIIG* gene and the *xylA* promoter region (from positions −256 to −1 relative to the transcriptional start site) were amplified separately, from chromosomal DNA of *B. subtilis* MB24. Primers P_{xylA}-*spoIIIG* and *spoIIIG*-2385R were used for the *spoIIIG* gene, and primers P_{xylA}D and P_{xylA}R were used for the *xylA* gene (Table 2). The 370-bp *spoIIIG* fragment was mixed with the 256-bp *xylA* fragment, and the resulting fragment of 619 bp was amplified using primers P_{xylA}D and *spoIIIG*-2385R. The P_{xylA}-*spoIIIG* fragment was digested with EcoRI and BamHI and ligated to similarly cut pDG364 (4), to yield pMS237. Strains AH3786 and AH3787 (Table 1) were transformed with BamHI-linearized pMS237, selecting for Cm^r/Sp^r cells, to yield strains AH2490 and AH2491, which carry a fusion of the xylose-inducible P_{xylA} promoter to the *spoIIIG* and *spoIIIGE156K* alleles at *amyE*, respectively (abbreviated to P_{xylA}-*spoIIIG* and P_{xylA}-*spoIIIGE156K*, respectively) (Table 1).

Fusion of the *spac* promoter to the *spoIIAB* gene. The *spoIIAB* gene was PCR amplified from the chromosomal DNA of strain MB24, using primers *spoIIAB*-166D and *spoIIAB*-665R (Table 2). The 499-bp *spoIIAB* fragment was digested with BamHI and SpeI and introduced between the BglII and SpeI sites of pDH88 (12), to yield pMS236. Next, a 2,189-bp EcoRI-to-BamHI fragment released from pMS236 was inserted between the same sites of pDG1664 (9), to generate pMS238. Strains AH2490 and AH2491 (Table 1) were transformed with XhoI-linearized pMS238 selecting for erythromycin resistance (Er^r), to yield AH2492 and AH2493, respectively, which carry a fusion of the P_{spac} promoter to *spoIIAB* inserted at the *thrC* locus (Δ*thrC*::P_{spac}-*spoIIAB*, abbreviated to P_{spac}-*spoIIAB*) (Table 1).

Fusions of *spoIIIG* to different sporulation promoters. Fusions of *spoIIIG* to the *spoIIQ* and to the *spoIID* promoters were constructed as follows. Initially, the 5′ end of the *spoIIIG* gene and its promoter region were amplified separately from chromosomal DNA of a wild-type *B. subtilis* strain. The following primers were used (Table 2): for *spoIIIG*, *spoIIIG-spoIIQ*, and *spoIIIG-spoIID*, primers *spoIIIG*-761R and *spoIIIG*-2385R; for *spoIIQ*, primers *spoIIQ*-152D and *spoIIQ*-500R; for *spoIID*, primers *spoIID*-1D and *spoIID*-500R. The 370-bp *spoIIIG* fragment was mixed with the 350-bp *spoIIQ* fragment or with the 500-bp *spoIID* fragment, and the resulting fragments of 720 and 870 bp were amplified using primers *spoIIQ*-152D and *spoIIIG*-761R for P_{spoIIQ}-*spoIIIG* or primers *spoIID*-1D and *spoIIIG*-2385R for P_{spoIID}-*spoIIIG*. The P_{spoIIQ}-*spoIIIG* fragment was digested with EcoRI and BglII and ligated to pDG364 (4) digested with EcoRI and BamHI to yield pMS134. The P_{spoIID}-*spoIIIG* fragment was digested with EcoRI and BamHI and ligated to similarly cut pDG364 (4) to yield pMS162. Strain AH3786 (Table 1) was transformed with pMS134 or pMS162 selecting for Cm^r/Sp^r cells, to yield AH3788 and AH2460, respectively. AH3787 (Table 1) was also transformed with pMS134 and pMS162 to yield the Cm^r/Sp^r strains AH3789 and AH2461, respectively. Fusion of the *spoIIIG* gene to the *spoIIQ* promoter and to the *spoIID* promoter by a double-crossover event at *amyE* was verified by PCR; the fusion alleles are abbreviated to P_{spoIIQ}-*spoIIIG* and P_{spoIID}-*spoIIIG*. Strain AH2462 was constructed by transformation of AH2452 (Δ*spoIIIG sspE-lacZ* [see above]) with DNA from AH2464 (Δ*lonA*::*cat*) (Table 1). Last, AH2462 was transformed with chromosomal DNA from AH2460 or AH2461 to produce AH2463 and AH2465, respectively (Table 1).

Immunoblotting. *B. subtilis* whole-cell lysates were prepared and Western blot analysis was performed as described previously (41).

β-Galactosidase assays. β-Galactosidase activity was assayed with the substrate *o*-nitrophenol-β-D-galactopyranoside (ONPG), and enzyme activity was expressed in Miller units as described previously (13).

Fluorescence microscopy. Immunofluorescence microscopy was conducted essentially as described previously (11, 33) except that a non-cross-linking fixative, Histochoice (Amresco, Solon, Ohio) was used. Immunolabeling was performed with rabbit polyclonal antibodies against β-galactosidase (Eppendorf–5 Prime, Inc., Boulder, Colo.) at a 1:1,000 dilution. A secondary antibody conjugated to Alexa Fluor 488 (Molecular Probes, Eugene, Oreg.) was used at a 1:500 dilution. To assess the completion of the engulfment process (morphological stage III of sporulation) (31), samples (0.5 ml) of DSM cultures were collected throughout sporulation and resuspended in the same volume of phosphate-buffered saline (8 mM sodium phosphate [pH 7.5], 150 mM NaCl) supplemented with FM-4-64 (5 μg/ml), 4′,6-diaminodino-2-phenylindole (DAPI) (0.2 μg/ml), and Mitotracker green FM (MTG) (15 μg/ml) (44). Cells were scored as having reached stage III when the membrane-impermeable stain FM4-64 (but not MTG) was excluded from the prespore membrane (44). In immunofluorescence experiments, the pattern of nucleoid staining with DAPI was used as an indication of the sporulation stage: just after formation of the asymmetric septum, the prespore nucleoid appears highly condensed, whereas soon after conclusion of the engulfment process, the mother cell and prespore nucleoids appear equally condensed (11, 43). Samples were observed in a Leica fluorescence microscope (DMRA2) using Leica filters A4, L5, and N3. All samples were observed with a 63x objective lens. Images were acquired with a Cool Snap HQ camera (Roper Scientific, Tucson, Ariz.) and recorded and processed for publication using Adobe Photoshop.

RESULTS

Isolation and characterization of the *spoIIIGE156K* allele. To analyze the mechanism by which σ^G is kept inactive in cells of a *spoIIIA* mutant, we sought random mutations in *spoIIIG* at *amyE* that bypassed the requirement for *spoIIIA* for expression of the σ^G-controlled *sspE-lacZ* fusion (26) (see Materials and Methods). We isolated one Lac^+ mutant called AH3791 (Table 1) upon transformation of *B. subtilis* strain AH2456 (Δ*spoIIIG spoIIIA*::Tn*917 sspE-lacZ*) with DNA from strain AH1843 mutagenized by *N*-methyl-*N*′-nitro-*N*-nitrosoguanidine (Table 1). Strain AH3791 harbored a single-nucleotide change (GAA to AAA) at codon 156 of the *spoIIIG* gene at *amyE* causing the replacement of a glutamic acid for a lysine. This allele of *spoIIIG* was designated *spoIIIGE156K*. Strains bearing a wild-type *spoIIIG* gene (AH3786) or the *spoIIIGE156K* allele (AH3787) at *amyE* in a *spoIIIG* mutant background (Δ*spoIIIG sspE-lacZ*) are Spo^+ (Table 3). Therefore, the *spoIIIGE156K* allele fully restored sporulation to a *spoIIIG* null mutant.

Expression of *sspE-lacZ* in *B. subtilis* strains AH3786 and AH3787 was induced around 4 h after the onset of sporulation (Fig. 1), as in a Spo^+ strain expressing the wild-type *spoIIIG* allele at its normal position (26; also data not shown), and reached maximum levels around 6 h after sporulation had started. As expected, expression of *sspE-lacZ* in strain AH3790 (Δ*spoIIIG spoIIIA*::Tn*917 sspE-lacZ* Δ*amyE*::*spoIIIG*) was severely impaired (19). However, in the congenic strain AH3791, which bears the *spoIIIGE156K* allele at *amyE*, expression of *sspE-lacZ* was restored (Fig. 1). Nevertheless, while in the $spoIIIA^+$ strain AH3787, expression of *sspE-lacZ* was strongly induced around 4 h after the onset of sporulation, in the *spoIIIA* mutant strain AH3791 (*spoIIIGE156K*), β-galactosidase accumulated at a reduced rate between 4 and 6 h after the onset of sporulation and reached maximum levels only around 10 h after sporulation had started (Fig. 1). Also, even though the *spoIIIGE156K* allele restores σ^G activity to *spoIIIA* cells, strain AH3791 was still unable to sporulate (Table 3). We also found that the *spoIIIGE156K* allele restored *sspE-lacZ* expression (but not sporulation) to a Δ*spoIIIJ*::*km* mutant (data not shown).

To investigate whether the increased activity of σ^{GE156K} in Spo^+ cells or in the *spoIIIA* mutant relative to wild-type σ^G could be attributed to its increased accumulation, we compared the levels of σ^G and σ^{GE156K} throughout sporulation by immunoblot analysis using a previously described anti-σ^G an-

TABLE 3. Sporulation of six *B. subtilis* strains

Strain	Relevant genotype	Sporulation[a]		% Sporulation
		Viable cells	Heat-resistant cells	
AH3786	*spoIIIG* $P_{spoIIIG}$-*spoIIIG*	6.9×10^8	5.0×10^8	72.5
AH3787	*spoIIIG* $P_{spoIIIG}$-*spoIIIGE156K*	5.0×10^8	3.8×10^8	76.0
AH3788	*spoIIIG* P_{spoIIQ}-*spoIIIG*	5.0×10^8	4.8×10^8	96.0
AH3789	*spoIIIG* P_{spoIIQ}-*spoIIIGE156K*	1.5×10^8	6.0×10^7	40.0
AH3790	*spoIIIG spoIIIA* $P_{spoIIIG}$-*spoIIIG*	1.4×10^8	3.0×10^4	0.02
AH3791	*spoIIIG spoIIIA* $P_{spoIIIG}$-*spoIIIGE156K*	1.1×10^8	1.0×10^4	0.01

[a] The extent of sporulation was measured 24 h after the onset of the process in liquid sporulation medium as described in Materials and Methods.

tibody (41). We found that in agreement with the timing of *sspE-lacZ* expression, σ^G or σ^{GE156K} reached peak levels around 4 h after the onset of sporulation in Spo$^+$ cells (Fig. 2A and B). In a *spoIIIA* background, the accumulation of the wild-type form of σ^G was delayed, reaching maximum levels around 6 h after the start of sporulation (Fig. 2C). In *spoIIIA*::Tn*917 spoIIIGE156K* cells (AH3791), σ^{GE156K} is detected only from 5 h on, and its accumulation reaches a maximum around 8 h after the onset of sporulation (Fig. 2D). The late accumulation of σ^{GE156K} in the *spoIIIA* mutant suggests that some σ^{GE156K} (but not wild-type σ^G) escapes inhibition late in sporulation and then amplifies its own synthesis. This late accumulation of σ^{GE156K} in the *spoIIIA*::Tn*917 spoIIIGE156K* double mutant correlates with the late expression of *sspE-lacZ* (Fig. 1). Note that under our electrophoretic conditions, the σ^{GE156K} form migrates slightly faster than wild-type σ^G (compare the mobility of σ^G and σ^{GE156K} relative to a background band labeled with an asterisk seen in a sample from a *spoIIIG* deletion mutant [Fig. 2A and B, for example]). The levels of σ^{GE156K} do not appear to be higher than those of wild-type σ^G in either *spoIIIA*$^+$ or *spoIIIA* mutant cells (Fig. 2, compare panels A and B and panels C and D). Thus, the difference in expression of *sspE-lacZ* in *spoIIIGE156K* strains AH3787 (*spoIIIA*$^+$) and AH3791 (*spoIIIA* mutant) relative to congenic strains expressing a wild-type *spoIIIG* gene at the *amyE* locus cannot be explained by an increase in the synthesis or stability of σ^G. Rather, it may reflect increased activity of the sigma factor. In the case of AH3791 (*spoIIIA*::Tn*917 spoIIIGE156K*), the increased activity of σ^{GE156K} is manifested only at a late time in development.

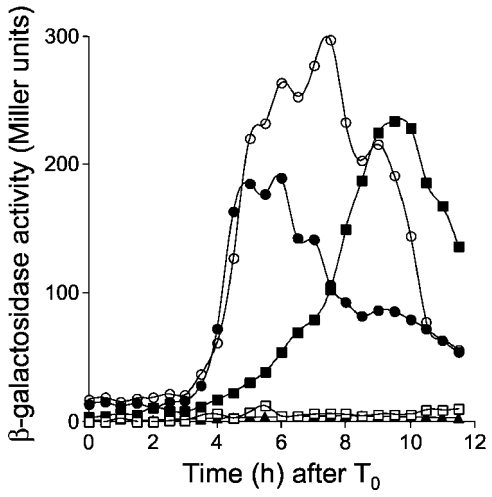

FIG. 1. The *spoIIIGE156K* allele bypasses the need for *spoIIIA* expression for σ^G activity. Expression of *sspE-lacZ* was monitored during sporulation in *B. subtilis* strains AH3786 (Δ*spoIIIG sspE-lacZ* Δ*amyE*::*spoIIIG*) (wild-type *spoIIIG* in a wild-type background) (closed circles), AH3787 (Δ*spoIIIG sspE-lacZ* Δ*amyE*::*spoIIIGE156K*) (open circles), AH3790 (Δ*spoIIIG sspE-lacZ spoIIIA*::Tn*917* Δ*amyE*::*spoIIIG*) (wt) (open squares), and AH3791 (Δ*spoIIIG sspE-lacZ spoIIIA*::Tn*917* Δ*amyE*::*spoIIIGE156K*) (closed squares). The complete relevant genotypes of the strains are given in Table 1. Strains were grown in DSM, and samples were taken at the indicated times (in hours) after the onset of sporulation (T_0) and assayed for β-galactosidase activity. Endogenous levels of β-galactosidase activity were determined in the wild-type strain MB24 (closed triangles). β-Galactosidase activity is given in Miller units (see Materials and Methods).

The E156K mutation is likely to interfere with the interaction between SpoIIAB and σ^G. Like *spoIIIGE156K*, a previously described allele of *spoIIIG* bearing a glutamate-to-lysine substitution at position 155 (*spoIIIGE155K*) allows expression of *sspE-lacZ* in cells with the mutant *spoIIIA* or *spoIIIJ* gene (19, 41). The E155K substitution was introduced in σ^G, because a glutamic acid-to-lysine substitution at an equivalent position of σ^F (E149K) was found in a genetic screen for σ^F mutants with reduced affinity for SpoIIAB (5). Moreover, under conditions in vitro that promote binding of SpoIIAB to σ^F, the anti-sigma factor also binds to σ^G, but not to σ^{GE155K} (19).

The binding of SpoIIAB to σ^F or σ^G can now be described in molecular terms, using the crystal structure (2) of the SpoIIAB-σ^F complex from *B. stearothermophilus* and the comparative models for the SpoIIAB-σ^F and SpoIIAB-σ^G complexes from *B. subtilis* derived here. These structures show that in *B. stearothermophilus* σ^F, the residue (E147) equivalent to E149 in the σ^F protein of *B. subtilis*, as well as three other residues found in genetic screens for mutants resistant to inhibition by SpoIIAB are located within a region that contains 17 amino acids (in *B. stearothermophilus*) found to interact with SpoIIAB (2, 5) (Fig. 3A to C). Of the amino acids, 15 are either identical or homologous in σ^G (compare Fig. 3, panels C and F) and 3 are uniquely conserved between σ^F and σ^G (2; also data not shown).

The nature of the E155K and E156K mutations in σ^G from *B. subtilis* can be qualitatively understood by examination of the model for the SpoIIAB-σ^G complex (Fig. 3D to F). The model shows that residue E155 of σ^G interacts with S17 in one of the SpoIIAB molecules present in the dimer (Fig. 3D to F and insert), a contact that is also conserved in the SpoIIAB-σ^F

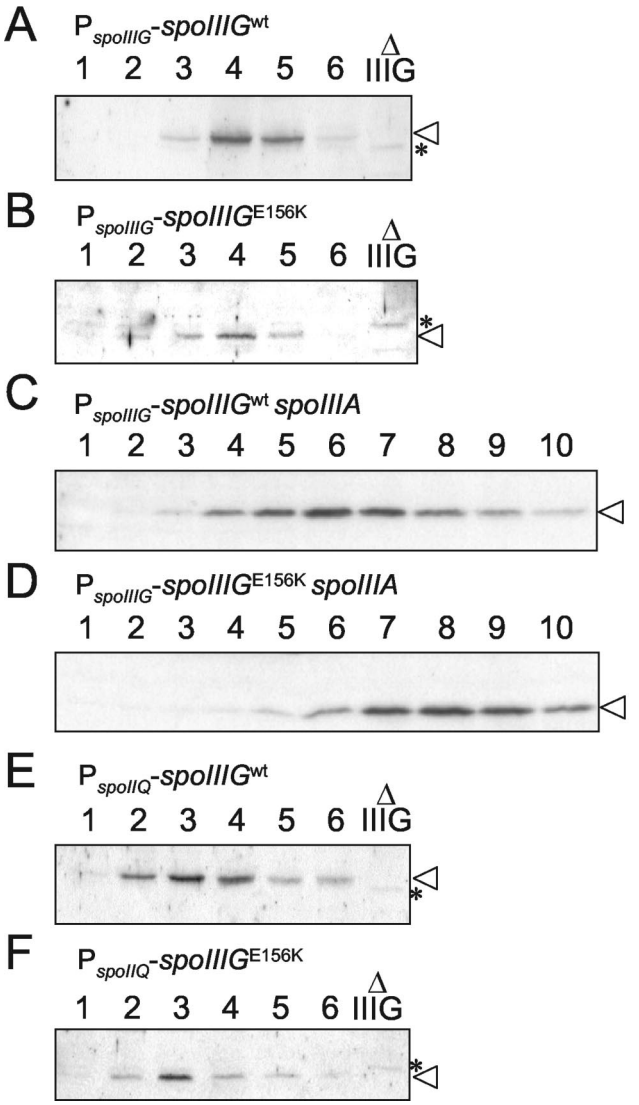

FIG. 2. Immunoblot analysis of σ^G accumulation during sporulation. σ^G accumulation in *B. subtilis* strains AH3786 (Δ*spoIIIG sspE-lacZ* Δ*amyE*::*spoIIIG*) (wild-type *spoIIIG* in a wild-type background) (A), AH3787 (Δ*spoIIIG sspE-lacZ* Δ*amyE*::*spoIIIGE156K*) (B), AH3790 (Δ*spoIIIG sspE-lacZ spoIIIA*::Tn*917* Δ*amyE*::*spoIIIG*) (wt) (C), AH3791 (Δ*spoIIIG sspE-lacZ spoIIIA*::Tn*917* Δ*amyE*::*spoIIIGE156K*) (D), AH3788 (Δ*spoIIIG sspE-lacZ* P_{spoIIQ}-*spoIIIG*) (wt) (E), and AH3789 (Δ*spoIIIG sspE-lacZ* P_{spoIIQ}-*spoIIIGE156K*) (F) during sporulation in DSM was examined by immunoblot analysis. The complete relevant genotypes of strains are given in Table 1. Samples from sporulating cultures were collected 1 h after the onset of sporulation in DSM and at hourly intervals thereafter, as indicated by the numbers above the lanes. Proteins (30 μg) in each sample were subjected to immunoblot analysis using an anti-σ^G rabbit polyclonal antibody (see Materials and Methods). Lanes Δ IIIG in panels A, B, E, and F contain 30-μg portions of an extract prepared from a *spoIIIG* deletion mutant (AH3795 [Table 1]) 4 h after the onset of sporulation in DSM (note that the *spoIIIG* deletion control was not included in panels C and D due to space limitations). The position of σ^G is indicated by an arrowhead. Other bands represent nonspecific cross-reactive material. One band seen in the *spoIIIG* deletion mutant is marked with an asterisk for reference.

complex (E149) (Fig. 3A to C). The models also predict that residue E156 of σ^G contacts residue K41 in the same SpoIIAB molecule contacted by residue E155 of σ^G (Fig. 3, insert), and again, this contact is conserved in the SpoIIAB-σ^F complex (D150) (Fig. 3A to C). Therefore, both the E155K and E156K substitutions introduce unfavorable interactions expected to destabilize the interaction of SpoIIAB with σ^G. We infer that the E156K mutation reduces the binding of SpoIIAB to σ^G in a manner similar to that observed for σ^{GE155K} (19). However, the interaction of E155 with a serine residue (S17) from SpoIIAB is likely to be less strong than the interaction of E156 that forms a salt bridge with K41 from SpoIIAB (Fig. 3, insert). Therefore, the effect of the E156K mutation, placing two positively charged residues in close proximity would create packing problems, and appears more disadvantageous for complex formation than the E155K mutation. Since the models for the two complexes show that most of the contacts between SpoIIAB and σ^F or σ^G are conserved, our analysis supports the conclusion of Evans et al. that the interaction of SpoIIAB with either σ^F or σ^G is very similar (7).

σ^{GE156K} is less sensitive to SpoIIAB in vivo. To determine whether the σ^{GE156K} form was less sensitive to the inhibitory action of SpoIIAB in vivo, we constructed strains engineered to coexpress *spoIIAB* and either *spoIIIG* or *spoIIIGE156K* during vegetative growth in a medium (LB) that does not support efficient sporulation. Strains AH2492 and AH2493 carry a fusion of the xylose-inducible P_{xylA} promoter to the *spoIIIG* and *spoIIIGE156K* genes, respectively, inserted at the *amyE* locus, as well as an IPTG-inducible P_{spac}-*spoIIAB* fusion inserted at the *thrC* locus; in addition, the two strains carry an *sspE-lacZ* fusion (Table 1). Preliminary experiments revealed that expression of P_{xylA}-*spoIIIG* and P_{xylA}-*spoIIIGE156K* in the absence of xylose resulted in significant expression of *sspE-lacZ* (data not shown). Therefore, AH2492 and AH2493 were grown in the absence of xylose and in the absence or presence of IPTG (1 mM) to induce SpoIIAB production.

Expression of *spoIIIG* or *spoIIIGE156K* in the presence or absence of SpoIIAB did not result in any detectable growth differences between the strains (Fig. 4A). The *sspE-lacZ*-driven production of β-galactosidase was monitored in the various cultures during the log phase of growth, 1.5, 2, and 2.5 h after inoculation. We found that in the absence of IPTG, the activities of both σ^G and σ^{GE156K} increased during the experiment, even though the activity of σ^{GE156K} was always lower than that of the wild-type form (Fig. 4B). In the presence of IPTG to induce *spoIIAB* expression, the activity of wild-type σ^G was immediately reduced and remained at low levels (Fig. 4B). In contrast, the activity of σ^{GE156K} was reduced slowly (Fig. 4B). Moreover, at all the times tested, the fraction of σ^{GE156K} activity remaining after IPTG-induced SpoIIAB synthesis was higher than the fraction of σ^G activity remaining after SpoIIAB induction (Fig. 4C). These results are consistent with the suggestion that the E156K substitution makes σ^G less sensitive to the inhibitory action of SpoIIAB.

Activity of σ^{GE156K} in a *spoIIIA* background is delayed relative to completion of the engulfment process. On the basis of an analogy to the E155K mutation and the results discussed above, we expected that the E156K substitution would also relieve the inhibitory action of SpoIIAB on σ^G during sporulation. If the interaction of SpoIIAB with σ^G were reduced, as

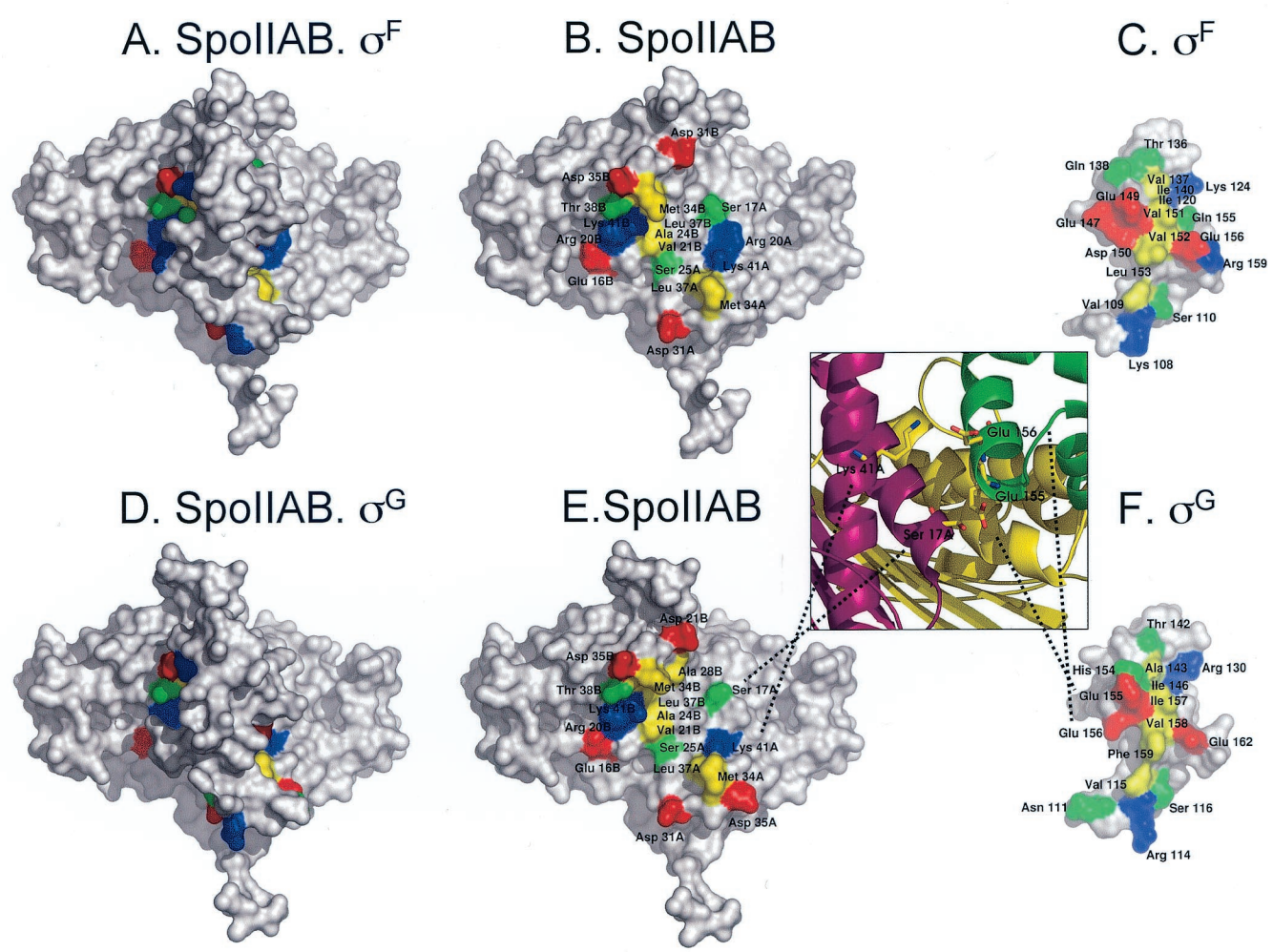

FIG. 3. Structures of the SpoIIAB-σ^F and SpoIIAB-σ^G complexes obtained by comparative modelling techniques. Panels A and D depict the whole complex between SpoIIAB and σ^F or σ^G, respectively, whereas panels B and E depict only SpoIIAB to display the residues from this protein that contact σ^F or σ^G. Panels C and F represent σ^F or σ^G, respectively, rotated 180° relative to the complexes shown in panels A and D, to display the contact residues from the σ factors. The positions of all contact residues are labeled. Since SpoIIAB is a dimer, the chain (A or B) of the contact residue is also identified. The structures are rendered using colored molecular surfaces generated using PyMOL (W. L. DeLano, The PyMOL Molecular Graphics System [2002], DeLano Scientific, San Carlos, Calif., http://www.pymol.org). Contact residues between σ^F or σ^G and SpoIIAB are colored according to their type; positively charged residues are blue, negatively charged residues are red, polar residues are green, and hydrophobic residues are yellow. The noncontacting surface is white. The insert between panels E and F is an expanded view of the interacting zone of residues E155 and E156 from σ^G in the SpoIIAB-σ^G complex. The proteins are represented using cartoons, colored differently to identify them (chains A and B from SpoIIAB are magenta and yellow, respectively, while σ^G is green).

suggested by our screen, and because σ^G is autoregulatory (17, 47), we would expect premature expression of *sspE-lacZ* if SpoIIAB were the primary inhibitor of σ^G activity in the prespore. In contrast to this expectation, activity of σ^{GE156K} was delayed in *spoIIIA* cells (Fig. 1), which remained unable to sporulate (AH3791) (Table 3).

To determine whether expression of *sspE-lacZ* was still coupled to the completion of the engulfment process in strain AH3791 (*spoIIIA spoIIIGE156K*), we used the membrane stains FM4-64 and MTG to monitor completion of the engulfment process (44). We stained samples of the same strains depicted in Fig. 1, and in parallel, we monitored accumulation of β-galactosidase to control for the onset of σ^G activity. We could not use a fusion of the *sspE* promoter to the *gfp* gene for this purpose, because even in the absence of σ^G, most of the cells showed some prespore decoration, presumably due to the activity of σ^F (data not shown).

As in the experiment documented in Fig. 1, expression of *sspE-lacZ* in the Spo$^+$ strains AH3786 (*spoIIIG* at *amyE*) and AH3787 (*spoIIIGE156K* at *amyE*) commenced around 4 h after the onset of sporulation, when 42 and 31% of the cells, respectively, had completed the engulfment process (Table 4). Activity of β-galactosidase peaked 6 h after the onset of sporulation for strain AH3786, when 48% of the cells showed complete engulfment of the prespore, and 6 to 8 h after the start of sporulation for AH3787, when 51 to 74% of the cells had completed the engulfment process (Table 4). These observations are in agreement with the results of a previous study,

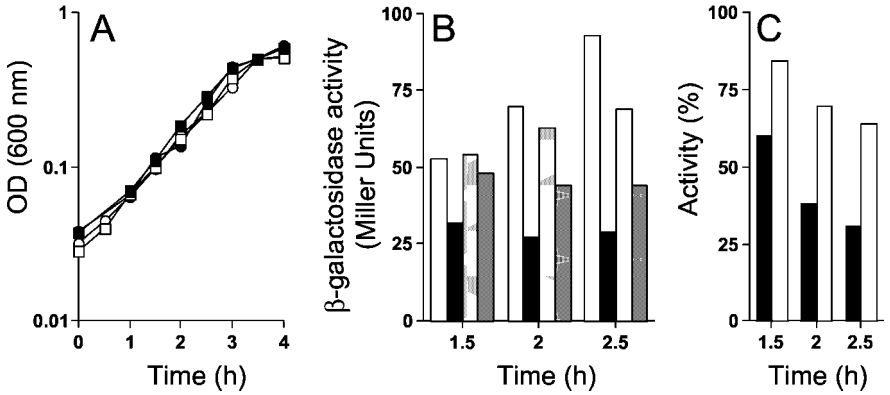

FIG. 4. σ^{GE156K} is less susceptible to SpoIIAB in vivo than wild-type σ^G. (A) *B. subtilis* strains AH2492 (P_{xylA}-*spoIIIG* P_{spac}-*spoIIAB sspE-lacZ*) (circles) and AH2493 (P_{xylA}-*spoIIIGE156K* P_{spac}-*spoIIAB sspE-lacZ*) (squares) were grown in LB medium with 1 mM IPTG (closed symbols) to induce *spoIIAB* expression or in the absence of inducer (open symbols). OD (600 nm), optical density at 600 nm. (B) Samples were taken at the indicated times and assayed for β-galactosidase production. From left to right, the four bars for each time point show the results for strain AH2492 grown in the absence of IPTG (white bars), AH2492 grown in the presence of IPTG (black bars), AH2493 grown in the absence of IPTG (light grey bars), and AH2493 grown in the presence of IPTG (dark grey bars). (C) Ratio between the activity of σ^G (black bars) or σ^{GE156K} (white bars) in the absence and presence of IPTG (expressed as a percentage).

suggesting that the activity of σ^G coincides with the completion of engulfment when sporulation is induced by growth and resuspension in a minimal medium (29). About 20% of AH3791 cells (*spoIIIA*::Tn*917 spoIIIGE156K*) showed complete engulfment by 4 h after the onset of sporulation, a fraction that increased to 39% by 6 h (Table 4), and by 8 h after sporulation had started, the number of cells showing clear signs of having completed the engulfment sequence reached a maximum of 54% (Table 4). However, this did not correspond to peak levels of *sspE-lacZ* expression (Fig. 1). Rather, enzyme production reached a maximum 10 h after the onset of sporulation, when the fraction of cells with clear signs of complete engulfment actually decreased to about 35% (Table 4). The reasons for this decrease may reflect instability of the prespore in cells bearing a *spoIIIA* mutation (see below). Consistent with this interpretation, 10 h after the onset of sporulation in strains bearing a mutation in *spoIIIA*, the pattern of fluorescence decoration resulting from MTG staining tended to change from the ellipsoidal contour of the prespore to a more or less indistinct mass of fluorescence, suggesting coalescence of the prespore membranes (data not shown). We note that a *spoIIIA* mutation per se does not significantly interfere with the timing of engulfment (AH3790) (Table 4). We interpret these observations as indicating that σ^{GE156K} becomes active only about 2 h after the completion of engulfment in a *spoIIIA* mutant.

TABLE 4. Time of engulfment completion in four *B. subtilis* strains

Strain	Genotype	Time (h)[a]	No. counted[b]	Sporulating cells/%[c]	Stage III cells/%[d]
AH3786	*spoIIIG* wt[e]	2	279	91/33	0
		4	143	101/71	60/42
		6	132	90/68	64/48
		8	131	100/76	86/66
		10	115	93/81	83/72
AH3787	*spoIIIGE156K*	2	487	153/31	0
		4	178	121/68	55/31
		6	357	221/62	53/51
		8	158	133/84	117/74
		10	172	129/75	114/66
AH3790	*spoIIIA spoIIIG* wt	2	157	70/45	0
		4	172	121/70	54/31
		6	167	119/71	98/59
		8	102	70/69	53/52
		10	152	67/44	48/32
AH3791	*spoIIIA spoIIIGE156K*	2	219	77/35	0
		4	260	110/42	50/20
		6	135	87/64	52/39
		8	111	76/68	60/54
		10	153	70/46	54/35

[a] Hours after the onset of sporulation.
[b] The total number of cells counted is indicated.
[c] The number of sporulating cells, estimated on the basis of the pattern of staining by FM4-64 and MTG (see text), is shown before the slash, and the percentage of sporulating cells is shown after the slash.
[d] The number of cells in stage III or above is shown before the slash, and the percentage of cells in stage III or above is shown after the slash.
[e] *spoIIIG* wt, wild-type *spoIIIG*.

Activity of σ^{GE156K} in a *spoIIIA* background is not confined to the prespore. The observation that the activity of σ^{GE156K} was delayed relative to the completion of the engulfment process in a *spoIIIA* mutant led us to examine the location of β-galactosidase produced from the *sspE-lacZ* fusion in this strain. We used immunofluorescence microscopy to examine samples of the same cultures used in the experiment depicted in Fig. 1 6 and 10 h after the onset of sporulation, as this corresponds to peak levels of *sspE-lacZ* expression in *spoIIIA*$^+$ or *spoIIIA* mutant cells, respectively (Fig. 1). We were unable to collect reasonable phase-contrast images or images of cells in which the membrane had been stained with FM4-64 or MTG after fixation and permeabilization of the cells with lysozyme (also see reference 33). For that reason, the number of sporulating cells was scored on the basis of the analysis of the pattern of nucleoid staining by DAPI (see Materials and Methods), and for each of these cells, the pattern of β-galactosidase localization was recorded (see Materials and Methods) (Table 5).

In strains AH3786 (Δ*spoIIIG sspE-lacZ* Δ*amyE*::*spoIIIG*) and AH3787 (Δ*spoIIIG sspE-lacZ* Δ*amyE*::*spoIIIGE156K*),

TABLE 5. Patterns of β-galactosidase localization

Strain	Genotype	Time (h)[a]	No. counted[b]	Sporulating cells/%[c]	Localization of β-galactosidase[d]		
					Prespore	MC	Whole cell
AH3786	*spoIIIG* wt	6	411	250/61	187	0	0
		10	360	358/99	9	0	0
AH3787	*spoIIIGE156K*	6	446	305/68	222	0	9
		10	413	397/96	10	0	3
AH3790	*spoIIIA spoIIIG* wt	6	193	151/78	0	0	0
		10	178	107/60	1	0	0
AH3791	*spoIIIA spoIIIGE156K*	6	431	309/75	0	2	12
		10	587	187/32	0	1	135

[a] Hours after the onset of sporulation.
[b] The total number of cells counted is indicated.
[c] The number of sporulating cells, estimated on the basis of the pattern of DAPI staining (see text), is shown before the slash, and the percentage of sporulation is shown after the slash.
[d] The number of cells or free spores in prespores, mother cells (MC), and whole cells (cells with no signs of prespore).

production of β-galactosidase was detected only in cells in which the prespore had been completely engulfed by the mother cell (as defined by DAPI staining, which reveals two equal-size mother cell and prespore chromosomes). Production of the enzyme was always confined to the prespore compartment of strain AH3786 (Fig. 5a to c and Table 5), whereas for strain AH3787, a small percentage of cells (around 1 or 2%) 6 or 10 h after the onset of sporulation showed fluorescence throughout the entire cell (Fig. 5f and Table 5). Interestingly, these specimens did not present any distinctive signs of sporulation as judged from the pattern of DAPI staining (Fig. 5d to f). This effect does not seem to be caused by deficient staining of one of the chromosomes, since the fluorescence signal is distributed by what would be the length of the entire sporulating cell (mother cell plus prespore). These specimens may represent vegetative cells or cells in which the normal compartmentalization of σ^G activity was lost (see below).

In agreement with the results of *sspE-lacZ* expression shown in Fig. 1, essentially no β-galactosidase could be detected in cells of AH3790 (Δ*spoIIIG spoIIIA*::Tn*917 sspE-lacZ* Δ*amyE*::*spoIIIG*) (Fig. 5i shows the only specimen found with signs of fluorescence in the prespore) (Table 5). About 3% of the cells of AH3791 (Δ*spoIIIG spoIIIA*::Tn*917 sspE-lacZ* Δ*amyE*::*spoIIIGE156K*) at 6 h after the onset of sporulation showed accumulation of β-galactosidase, a percentage that increased to 23% at 10 h (Table 5). Surprisingly, in most of these cells, β-galactosidase was found to localize throughout the entire cell (Fig. 5j to l and Table 5). The percentage of sporulating cells of AH3791 (two visible nucleoids of about the same size at this stage) decreased from 75% at 6 h after the onset of sporulation to about 32% at 10 h (Fig. 5j to l [6 h] and m to o [10 h] and Table 5). Note that the specimens showing whole-cell fluorescence do not show the DAPI staining pattern of a mid to late stage of sporulation and that specimens in which the prespore can be clearly distinguished do not show *sspE-lacZ* expression (Fig. 5j to o). The percentage of AH3790 cells (wild-type *spoIIIG* in a *spoIIIA* background) with two distinct nucleoids also decreased from 6 h (78%) to 10 h after the onset of sporulation (60%) (Table 5) except that in the latter case, the whole-cell pattern of decoration was never found. No decrease in the percentage of sporulating cells was noticed for the *spoIIIA*$^+$ strains.

The results show that σ^{G156K} does not become active exclusively in the prespore of a *spoIIIA* mutant. The results suggest that *spoIIIA* may function to antagonize an as yet unknown negative regulator of σ^G following completion of the engulfment process and that *spoIIIA* may serve an additional function in sporulation related to the maintenance of compartmentalized gene expression in postengulfment cells. Essentially the same observations, i.e., absence of prespore-specific expression of *sspE-lacZ*, were made for *spoIIIA* cells harboring the E155K mutation (19; E. M. Kellner and C. P. Moran, Jr., unpublished results), reinforcing the view that the E155K and E156K substitutions affect the activity of σ^G similarly.

Early expression of *spoIIIGE156K* in the prespore does not result in premature activity of σ^G. Transcription of the *spoIIIG* gene by σ^G is delayed by an unknown mechanism towards the end of the engulfment process relative to the transcription of the first class of σ^F-dependent genes, which includes the *spoIIQ* gene (24). We fused the coding region of *spoIIIGE156K* to the early σ^F-dependent *spoIIQ* promoter, reasoning that the fusion allele would bypass both the mechanism that delays transcription of *spoIIIG* and a possible negative effect of SpoIIAB prior to engulfment. The promoter fusion was introduced at the *amyE* locus, producing strain AH3789 (Δ*spoIIIG sspE-lacZ* P_{spoIIQ}-*spoIIIGE156K*). The *spoIIQ* promoter was also fused to the coding region of the wild-type *spoIIIG* gene, and the fusion was inserted at *amyE* to produce AH3788 (Δ*spoIIIG sspE-lacZ* P_{spoIIQ}-*spoIIIG*). Both AH3789 and AH3788 sporulate efficiently (Table 3).

In agreement with unpublished work cited by Stragier and Losick (46), the expression of *sspE-lacZ* in AH3788 began to increase around 4 h after the onset of sporulation, as in strains bearing the wild-type or *spoIIIGE156K* allele under the control of its native promoter (AH3786 and AH3787) (Fig. 6). Moreover, induction of *sspE-lacZ* also occurred around 4 h of sporulation in strain AH3789 (Fig. 6); the *spoIIQ* promoter drives expression of *spoIIIGE156K* in AH3789.

When produced from their own promoter, σ^G and σ^{GE156K} were first detected 3 h after the onset of sporulation, and the

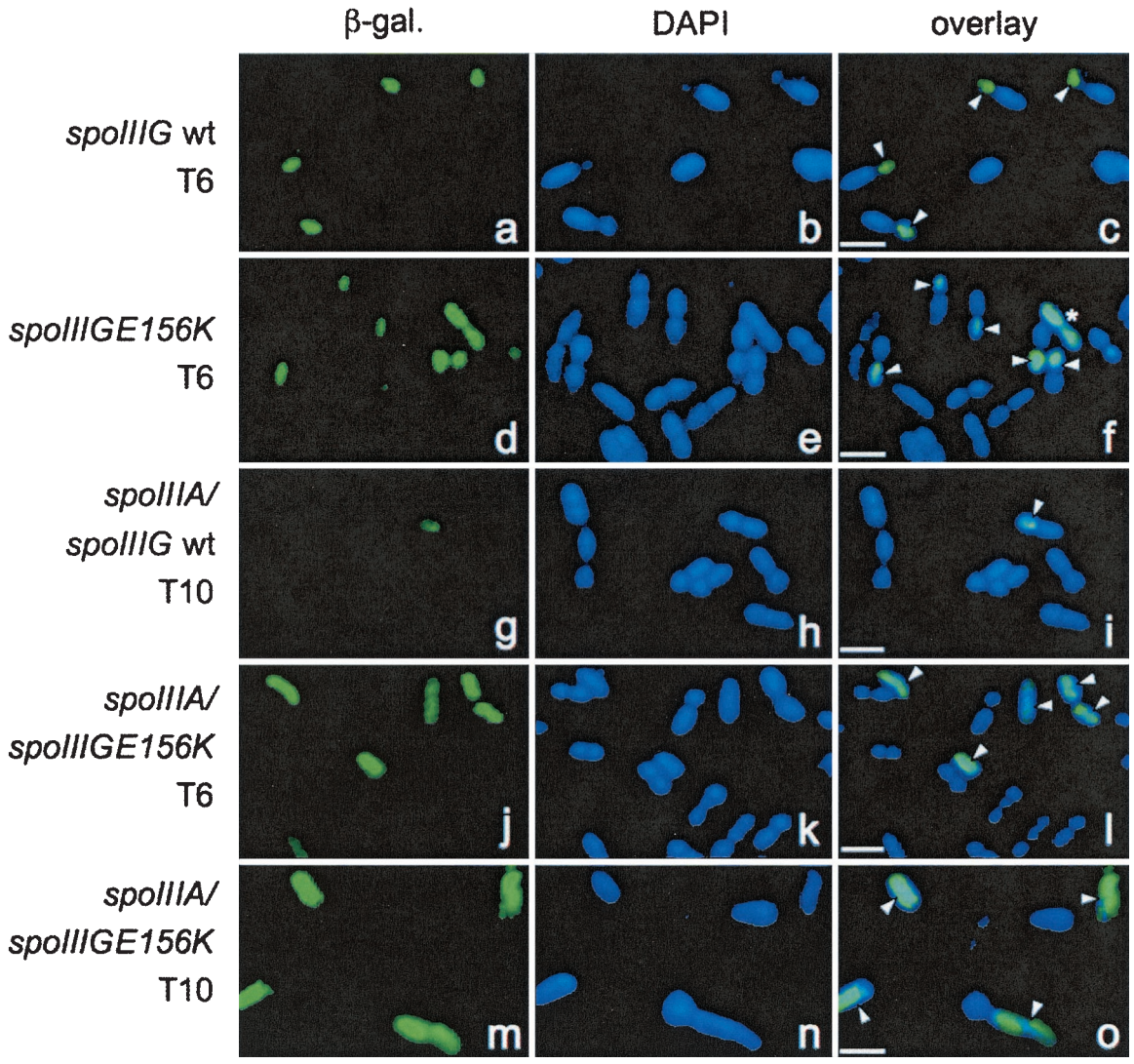

FIG. 5. Immunolocalization patterns of β-galactosidase produced from the *sspE-lacZ* fusion. The strains of *B. subtilis* were grown in DSM, and samples were taken at the indicated times after the onset of sporulation, stained with DAPI, and processed for immunofluorescence microscopy as described in Materials and Methods. Typical localization patterns of β-galactosidase (β-gal.) produced from the *sspE-lacZ* fusion for strains AH3786 (Δ*spoIIIG sspE-lacZ* Δ*amyE*::*spoIIIG*) (wild-type *spoIIIG* in a wild-type background) (a to c), AH3787 (Δ*spoIIIG sspE-lacZ* Δ*amyE*::*spoIIIGE156K*) (d to f), AH3790 (Δ*spoIIIG spoIIIA*::Tn*917 sspE-lacZ* Δ*amyE*::*spoIIIG*) (wt) (g to i), and AH3791 (Δ*spoIIIG spoIIIA*::Tn*917 sspE-lacZ* Δ*amyE*::*spoIIIGE156K*) (j to o) at the indicated times after the onset of sporulation are shown. The complete relevant genotypes of the strains are given in Table 1. The samples were taken 6 or 10 h after the onset of sporulation (T6 and T10, respectively). Arrowheads point to specimens showing *sspE-lacZ* expression. The specimen labeled with an asterisk in panel f, as well as the specimens in panels l and o, show whole-cell fluorescence (see text). Bars, 2 μm.

level of the σ^G factor increased until 4 h (Fig. 2A and B), whereas utilization of the *spoIIQ* promoter permitted the accumulation of σ^G or σ^{GE156K} from 2 h on, with maximum levels between 3 and 4 h after the onset of sporulation (Fig. 2E and F). In all the strains included in the experiment of Fig. 6, induction of s*spE-lacZ* expression 4 h after the onset of sporulation coincided with completion of the engulfment process (as assayed by FM4-64 or MTG staining) (between 31 and 56% [data not shown]). Both strains bearing the wild-type or *spoIIIGE156K* allele under the control of the *spoIIQ* promoter presented a high background of σ^G activity starting at the onset of sporulation. The reason for this behavior is not known, but it could be the result of high levels of expression of *spoIIIG* or *spoIIIGE156K* from the strong *spoIIQ* promoter (24). In any event, we note that expression of *spoIIIGE156K* does not result in a higher background relative to expression of the wild-type *spoIIIG* gene (Fig. 6). Moreover, we note that in both AH3788 and AH3789, expression of *sspE-lacZ* remains constant (Fig. 6), while the cellular levels of σ^G increase (Fig. 2E and F). It appears that even though σ^{GE156K} accumulates starting 2 h after the onset of sporulation, it directs induction of *sspE-lacZ* expression only around 4 h, when the process of engulfment of the prespore by the mother cell is complete. Together, the results suggest that SpoIIAB may not contribute decisively to

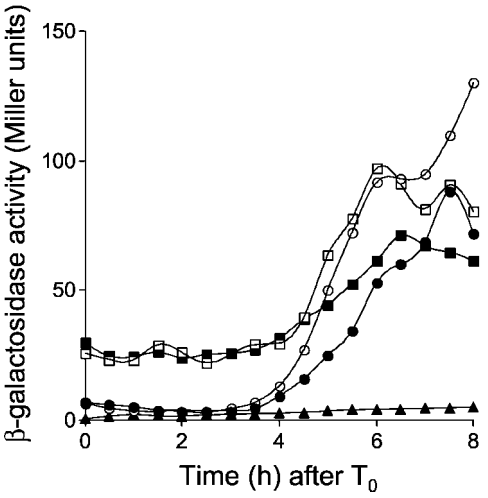

FIG. 6. Early expression of wild-type *spoIIIG* and *spoIIIGE156K* genes in the prespore. Expression of *sspE-lacZ* was monitored during sporulation in *B. subtilis* strains AH3786 (Δ*spoIIIG sspE-lacZ amyE*::*spoIIIG*) (wild-type *spoIIIG* in a wild-type background) (closed circles), AH3787 (Δ*spoIIIG sspE-lacZ* Δ*amyE*::*spoIIIGE156K*) (open circles), AH3788 (Δ*spoIIIG sspE-lacZ* P_{spoIIQ}-*spoIIIG*) (wt) (open squares), and AH3789 (Δ*spoIIIG sspE-lacZ* P_{spoIIQ}-*spoIIIGE156K*) (closed squares). The complete relevant genotypes of strains are given in Table 1. Strains were grown in DSM, and samples were taken at the indicated times (in hours) after the onset of sporulation (T_0) and assayed for β-galactosidase activity. The endogenous levels of β-galactosidase activity were determined in the wild-type strain MB24 (closed triangles). β-Galactosidase activity is given in Miller units (see Materials and Methods).

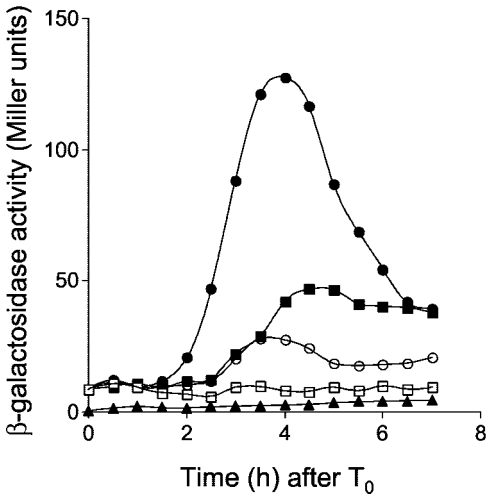

FIG. 7. Role of SpoIIAB in the regulation of σ^G activity in the mother cell. Expression of *sspE-lacZ* was monitored during sporulation in *B. subtilis* strains AH2460 (Δ*spoIIIG sspE-lacZ* P_{spoIID}-*spoIIIG*) (wild-type *spoIIIG* in a wild-type background) (open squares), AH2461 (Δ*spoIIIG sspE-lacZ* P_{spoIID}-*spoIIIGE156K*) (closed squares), AH2463 (Δ*spoIIIG sspE-lacZ lonA*::*cat* P_{spoIID}-*spoIIIG*) (wt) (open circles), and AH2465 (Δ*spoIIIG sspE-lacZ lonA*::*cat* P_{spoIID}-*spoIIIGE156K*) (closed circles). The complete relevant genotypes of strains are given in Table 1. Strains were grown in DSM, and samples were taken at the indicated times (in hours) after the onset of sporulation (T_0) and assayed for β-galactosidase activity. The endogenous levels of β-galactosidase production were determined in the wild-type strain MB24 (closed triangles). β-Galactosidase activity is given in Miller units (see Materials and Methods).

the inhibition of σ^G activity in the prespore. The fact that very little free SpoIIAB seems to accumulate in the prespore and the similarity of the interaction of SpoIIAB with both σ^F and σ^G (7, 28; this work) are consistent with this interpretation.

Activity of σ^G in the mother cell is antagonized by SpoIIAB and LonA. Since σ^G is autoregulatory and SpoIIAB is present in both the prespore and mother cell compartments, we wanted to determine whether SpoIIAB could have a role in the negative regulation of σ^G in the mother cell, as previously suggested (3, 8, 19, 21, 35). To investigate this possibility, we fused the coding regions of the wild-type and *spoIIIGE156K* alleles to the mother cell-specific, σ^E-dependent *spoIID* promoter (36). The fusions were transferred to the *amyE* locus of a strain bearing an in-frame deletion of the *spoIIIG* gene and an *sspE-lacZ* fusion (AH2452), yielding strains AH2460 (Δ*spoIIIG sspE-lacZ* P_{spoIID}-*spoIIIG*) and AH2461 (Δ*spoIIIG sspE-lacZ* P_{spoIID}-*spoIIIGE156K*) (Table 1). No σ^G activity was detected by monitoring *sspE-lacZ*-driven β-galactosidase production, when the wild-type *spoIIIG* allele was expressed in the mother cell (Fig. 7). In contrast, expression of the *spoIIIGE156K* allele promptly resulted in *sspE-lacZ* expression, which occurred prior to normal expression of *sspE* in the prespore, in agreement with the timing of utilization of the *spoIID* and *sspE* promoters during sporulation (26, 36) (Fig. 7). This observation supports a role for SpoIIAB in the regulation of σ^G activity in the mother cell.

To determine whether the elevated levels of σ^G activity observed in strain AH2461 (P_{spoIID}-*spoIIIGE156K*) relative to strain AH2460 (P_{spoIID}-*spoIIIG*) correlated with increased accumulation of σ^G, we conducted immunoblot experiments. We found that the σ^{GE156K} protein accumulated starting 2 h after the onset of sporulation, reaching maximum levels around 3 h after sporulation had begun (Fig. 8B), which is in accordance with the temporal pattern of expression of a *spoIID-lacZ* fusion (36). In contrast, the wild-type form of σ^G was detected only in trace amounts (Fig. 8A), suggesting that σ^G is subjected to proteolysis in the mother cell.

Since the ATP-dependent LonA protease has been implicated in the negative regulation of σ^G (40, 42), we examined whether a mutation in the *lonA* gene would also result in increased σ^G activity in the mother cell. A Δ*lonA*::*cat* allele was introduced in strain AH2460, yielding strain AH2463 (Δ*spoIIIG sspE-lacZ* P_{spoIID}-*spoIIIG lonA*::*cat*) (Table 1). Like the *spoIIIGE156K* allele, the *lonA* mutation also permitted expression of *sspE-lacZ* (Fig. 7), and the strain accumulated wild-type σ^G starting 2 h after the onset of sporulation, with peak levels around 3 h after sporulation had begun (Fig. 8C). Even though the levels of wild-type σ^G in AH2463 (*lonA*) appeared higher than the levels of σ^{GE156K} in AH2461 (Fig. 8, compare panels B and C), the latter strain showed the highest levels of *sspE-lacZ* expression (Fig. 7), suggesting that σ^{GE156K} is still regulated by LonA.

To test this possibility, we introduced the Δ*lonA*::*cat* allele into strain AH2461, yielding strain AH2465 (Δ*spoIIIG sspE-lacZ* P_{spoIID}-*spoIIIGE156K lonA*::*cat*) (Table 1). Strain AH2465 showed higher levels of *sspE-lacZ* expression than AH2461 (*spoIIIGE156K*) (Fig. 7). Moreover, σ^{GE156K} accumulated at higher levels than in the *lonA*$^+$ strain AH2461 (Fig. 8B and D). These results show that the σ^{GE156K} form is only partially resistant to LonA. Since the levels of σ^{GE156K} in a

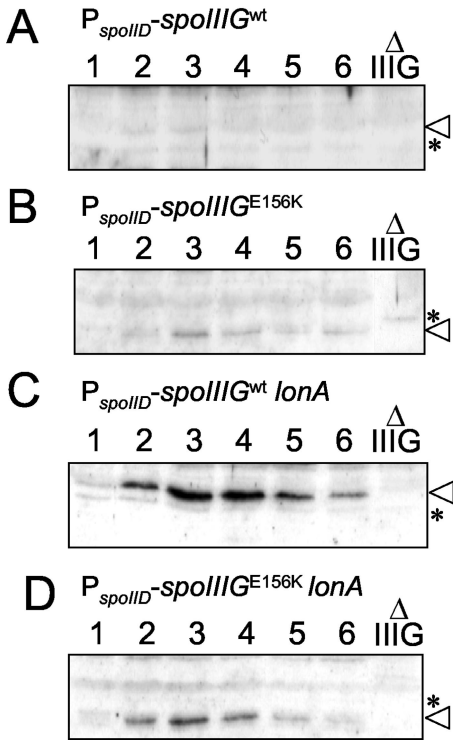

FIG. 8. Immunoblot analysis of σ^G accumulation produced in the mother cell during sporulation. σ^G accumulation in *B. subtilis* strains AH2460 (Δ*spoIIIG sspE-lacZ* P_{spoIID}-*spoIIIG*) (wild-type *spoIIIG* in a wild-type background) (A), AH2461 (Δ*spoIIIG sspE-lacZ* P_{spoIID}-*spoIIIGE156K*) (B), AH2463 (Δ*spoIIIG sspE-lacZ lonA*::*cat* P_{spoIID}-*spoIIIG*) (wt) (C), and AH2465 (Δ*spoIIIG sspE-lacZ lonA*::*cat* P_{spoIID}-*spoIIIGE156K*) (D) during sporulation in DSM was examined by immunoblot analysis. Samples from sporulating cultures were collected 1 h after the onset of sporulation in DSM and at hourly intervals thereafter, as indicated by the numbers above the lanes. Proteins (30 μg) in each sample were subjected to immunoblot analysis using an anti-σ^G rabbit polyclonal antibody (see Materials and Methods). Lanes Δ IIIG contain 30-μg portions of an extract prepared from a culture of a spo*IIIG* deletion mutant (AH3795 [Table 1]) 4 h after the onset of sporulation. The position of σ^G is indicated by an arrowhead. Other bands represent nonspecific cross-reactive material. One band, which appears close to σ^G in the *spoIIIG* deletion mutant, is marked with an asterisk for reference.

lonA background were lower than the levels of wild-type σ^G, the σ^{GE156K} form may be a substrate for yet another protease. These observations are in agreement with the reduced accumulation relative to wild-type σ^G in all backgrounds (Fig. 2 and 8). Together, the results suggest that σ^G does not normally accumulate to significant levels in the mother cell, because of the action of LonA and that in its absence, σ^G is still negatively regulated by SpoIIAB. Moreover, since the same form of σ^G (σ^{GE156K}) presumed to interact deficiently with the anti-sigma factor SpoIIAB is also partially resistant to LonA (Fig. 8B), the E156K substitution may protect σ^G from both SpoIIAB and LonA. In any event, the results suggest that both SpoIIAB and LonA contribute to the negative regulation of σ^G in the mother cell chamber of the sporulating cell.

DISCUSSION

Previous work has shown that σ^G accumulates but is mostly inactive in *spoIIIA* or *spoIIIJ* mutants of *B. subtilis* (19, 41), both of which show a morphological block just after completion of the engulfment process (6, 30). This has led to the suggestion that both *spoIIIA* and *spoIIIJ* act after engulfment to promote the activation of σ^G in the prespore. Since the activity of σ^G can be restored to *spoIIIA* or *spoIIIJ* mutants by a form of σ^G that is not efficiently bound by SpoIIAB in vitro, it has also been proposed that the expression of both loci would be required to antagonize the action of SpoIIAB upon completion of the engulfment process (19, 41). In this study, we have screened for random mutations in *spoIIIG* that could bypass the need for *spoIIIA* for expression of the σ^G-controlled *sspE* gene. We isolated a single allele of *spoIIIG* (*spoIIIGE156K*), which codes for lysine at position 156 of σ^G, instead of glutamate. On the basis of the analysis of a model of the complex between *B. subtilis* σ^G and a SpoIIAB dimer, we infer that this allele interferes with the interaction of σ^G with SpoIIAB by destroying the salt bridge between glutamate 156 of σ^G and lysine 41 in one of the SpoIIAB molecules (Fig. 3). The previously described E155K substitution (19) prevents the formation of a hydrogen bond between glutamate 155 of σ^G and serine 17 in SpoIIAB (Fig. 3). This suggests that σ^{GE156K} is at least as refractory to SpoIIAB binding as σ^{GE155K}. The reduced susceptibility of σ^{GE156K} to SpoIIAB compared to the susceptibility of wild-type σ^G in vegetative cells of *B. subtilis* is in agreement with the idea that the E156K mutation interferes with SpoIIAB binding (Fig. 4).

In wild-type cells, the prespore-specific activation of σ^G coincides with the completion of the engulfment process (29; this work). The main finding of this investigation was that expression of *sspE-lacZ* in cells of the *spoIIIA spoIIIGE156K* mutant was delayed relative to completion of engulfment and was not confined to the prespore compartment. In strain AH3791 (a *spoIIIA spoIIIGE156K* double mutant expressing *sspE-lacZ*), the fraction of cells that had completed engulfment 4 h after the onset of sporulation was half that observed for a wild-type strain, and by 6 h after the onset of sporulation, the proportion of AH3791 cells with fully engulfed prespores (39%) was even closer to that of the wild-type AH3786 (48%). However, in AH3791, the activity of β-galactosidase peaked at 10 h after the onset of sporulation, not at 6 h as in a wild-type strain (Fig. 1). Moreover, the peak of β-galactosidase activity in AH3791 did not coincide with an increase in the frequency of fully engulfed prespores but with a decrease in cells with clear signs of sporulation (Tables 4 and 5; see below).

In addition, β-galactosidase was not confined to the prespore but distributed throughout the entire cell (Fig. 5). The pattern of whole-cell decoration could represent cells that have not entered the sporulation pathway and maintain their vegetative state. Because σ^G is autoregulatory (17, 47) and because SpoIIAB negatively regulates σ^G in nonsporulating cells (8, 35), a mutation impairing SpoIIAB binding could result in increased activity of σ^G. In that case, σ^G activity should have been detected during growth, early in sporulation, and presumably also in the mother cell in strains bearing the *spoIIIGE156K* allele. However, this was not the case: no β-galactosidase accumulated during vegetative growth (data not shown), and very few cells of the Spo^+ strain AH3787 (which express *spoIIIGE156K* in a *spoIIIA*$^+$ background) presented the same pattern of whole-cell decoration (Fig. 5 and Table 5). An alternative explanation is that the whole-cell decoration

pattern corresponds to cells that have entered sporulation but that late in development they fail to maintain compartmentalized gene expression because the *spoIIIA* mutation results in instability of the prespore envelope. We favor this idea for two reasons. First, the instability of the prespore membranes has been reported for certain mutants that do not proceed past the stage of the completion of engulfment (30, 32). Second, it agrees with the observation that in cells bearing a *spoIIIA* mutation (expressing either the wild-type allele or *spoIIIGE156K*), the percentage of sporulation seems to decrease from 6 to 10 h after the onset of sporulation, as scored by the staining patterns of the prespore membranes by MTG (Table 4) and of the nucleoid by DAPI (Table 5). Thus, expression of *sspE-lacZ* in the *spoIIIA spoIIIGE156K* mutant (AH3791) would occur only upon partial lysis of the prespore at a late time in development, permitting access of some σ^{GE156K} to the mother cell, where it would prime its own synthesis. Note that σ^{GE156K} accumulates in the mother cell, whereas wild-type σ^G does not (Fig. 8; see below). The loss compartmentalization of σ^F activity in *spoIIIE* insertional mutants indicates that the prespore membranes become permeable to sigma factors at least under certain conditions (50).

Whatever the correct interpretation, the observation that the *spoIIIGE156K* allele does not restore prespore-specific expression of *sspE-lacZ* to a *spoIIIA* mutant has several implications. If mutations that impair binding of SpoIIAB do not permit activation of σ^G in the prespore of a *spoIIIA* mutant after completion of the engulfment process, then it seems likely that the activity of σ^G is negatively regulated by some other factor. It would be difficult to explain that SpoIIAB inhibits σ^G at a time when SpoIIAB is inactivated to permit expression of the σ^F regulon (reviewed in references 31 and 37), especially if the interaction of SpoIIAB with σ^F is similar to that of SpoIIAB with σ^G (7; this work). Moreover, because uncomplexed SpoIIAB is rapidly proteolyzed, there seems to be very little, if any, free SpoIIAB in the prespore (28). Normally, σ^G is produced late, just prior to the completion of the engulfment process (29). However, since σ^G efficiently recognizes its own promoter, even low levels of σ^G would have to be subjected to negative regulation. It could be that very low levels of SpoIIAB escaping proteolysis would be sufficient to maintain the inactivity of σ^G. This seems unlikely, because expression of the wild-type or *spoIIIGE156K* allele from the strong, early σ^F-dependent *spoIIQ* promoter does not result in premature induction of *sspE-lacZ* expression (46) (Fig. 6). Together, these observations suggest that σ^{G156K} is kept inactive in the prespore by an as yet unidentified factor, which is antagonized in the postengulfment prespore in a *spoIIIA*- and *spoIIIJ*-dependent manner. Since activity of σ^{GE156K} is detected in *spoIIIA* or *spoIIIJ* mutants only at late times after sporulation, when the prespore membranes show signs of instability, it is possible that the putative prespore inhibitor of σ^G is unstable and tends to disappear at late times in sporulation. We do not know whether σ^G is equally unstable, but presumably very little σ^G is needed to establish the positive-feedback loop leading to its increased accumulation around 8 h after the onset of sporulation (Fig. 2). The results suggest that SpoIIAB is either not involved in the regulation of σ^G in the prespore or is redundant. Since no mutations that result in deregulated σ^G activity in the prespore are known, it may be that the putative inhibitor of σ^G (if other than SpoIIAB) has remained elusive, because it is the product of a small or essential gene or because mutations that make σ^G resistant to inhibition also impair its activity.

Also worthy of comment is the role of SpoIIAB in the mother cell, together with the LonA protease. We found that the wild-type σ^G does not accumulate in the mother cell when expressed from the strong σ^E-dependent *spoIID* promoter (Fig. 8A). Because a mutation in the *lonA* gene, encoding the ATP-dependent LonA protease, results in accumulation of σ^G and expression of *sspE-lacZ*, LonA appears to promote the degradation of σ^G in the mother cell (Fig. 7 and 8C). Since expression of *spoIIIGE156K* from the *spoIID* promoter results in higher levels of *sspE-lacZ* expression, we conclude that SpoIIAB is also capable of inhibiting σ^G in the mother cell (Fig. 7). LonA has been previously implicated in the negative regulation of σ^G under nutritional conditions that do not allow efficient sporulation (40). Moreover, a mutation in the *lonA* gene is also able to partially restore σ^G activity to a *spoIIIA* mutant during sporulation but only after a delay of 2 h relative to the normal timing of expression of the σ^G regulon (40). This effect is reminiscent to that observed for the *spoIIIGE155K* or *spoIIIGE156K* allele, and it could be restricted to the mother cell, since expression of *lonA* from a prespore-specific promoter was found to strongly reduce σ^G activity and sporulation (42). In any event, since the E156K mutation also confers some immunity against LonA (Fig. 8B), at this time we cannot decide whether expression of *sspE-lacZ* in cells of the *spoIIIA*::Tn*917 spoIIIGE156K* double mutant (AH3791) is a consequence of the impaired ability of SpoIIAB to bind to σ^G, its resistance to the LonA protease, or both.

In conclusion, our results suggest that mutations that make σ^G resistant to SpoIIAB do not permit expression of the σ^G-dependent *sspE* gene in the prespore of a *spoIIIA* mutant. While our results support earlier findings indicating that SpoIIAB (together with LonA) is important in the mother cell, they suggest that SpoIIAB is not a decisive regulator of σ^G in the prespore.

ACKNOWLEDGMENTS

We thank Gonçalo Real and Patrick Piggot for helpful discussions and comments on the manuscript and Ellen Kellner and Patrick Piggot for sharing information prior to publication and for helpful discussions. We also thank Filipe Vieira for help with some of the plasmid constructions.

This work was supported in part by grants Praxis XXI/PCNA/C/BIO/13201/98 and PRAXIS/BIO/35109/99 from the Fundação para a Ciência e a Tecnologia (F.C.T.) to A.O.H and grant GM54395 from the National Institutes of Health to C. P. Moran, Jr. M.S. is the recipient of a Ph.D. fellowship (PRAXIS XXI/BD 18 251/98) from the F.C.T.

ADDENDUM IN PROOF

A recent report shows that compartmentalized gene expression is compromised in *spoIIIA* or *spoIIIJ B. subtilis* mutants because of prespore instability (Z. Li, F. Di Donato, and P. J. Piggot, J. Bacteriol. **186:**2221–2223, 2004). These results support our interpretation that the activity of σ^{GE156K} seen in *spoIIIA* cells is due to instability of the prespore and loss of compartmentalized gene expression in this mutant background.

REFERENCES

1. **Campbell, E. A., and S. A. Darst.** 2000. The anti-σ factor SpoIIAB forms a 2:1 complex with σ^F, contacting multiple conserved regions of the σ factor. J. Mol. Biol. **300:**17–28.

2. **Campbell, E. A., S. Masuda, J. L. Sun, O. Muzzin, C. A. Olson, S. Wang, and S. A. Darst.** 2002. Crystal structure of the *Bacillus stearothermophilus* anti-σ factor SpoIIAB with the sporulation factor σ^F. Cell **108:**795–807.
3. **Coppolechia, R., H. DeGrazia, and C. P. Moran, Jr.** 1991. Deletion of *spoIIAB* blocks endospore formation in *Bacillus subtilis* at an early stage. J. Bacteriol. **173:**6678–6685.
4. **Cutting, S. M., and P. B. V. Horn.** 1990. Genetics analysis, p. 27–74. *In* C. R. Harwood and S. M. Cutting (ed.), Molecular biological methods for *Bacillus*. John Wiley & Sons Ltd., Chichester, England.
5. **Decatur, A., and R. Losick.** 1996. Multiple sites of contact between the *Bacillus subtilis* developmental transcription factor σ^F and its anti-sigma factor SpoIIAB. Genes Dev. **10:**2348–2358.
6. **Errington, J., L. Appleby, R. A. Daniel, H. Goodfellow, S. R. Partridge, and M. D. Yudkin.** 1992. Structure and function of the *spoIIIJ* gene of *Bacillus subtilis*: a vegetatively expressed gene that is essential for sigma G activity at an intermediate stage of sporulation. J. Gen. Microbiol. **138:**2609–2618.
7. **Evans, L., J. Clarkson, M. D. Yudkin, J. Errington, and A. Feucht.** 2003. Analysis of the interaction between the transcription factor σ^G and the anti-sigma factor SpoIIAB of *Bacillus subtilis*. J. Bacteriol. **185:**4615–4619.
8. **Foulger, D., and J. Errington.** 1993. Effects of new mutations in the *spoIIAB* gene of *Bacillus subtilis* on the regulation of σ^F and σ^G activities. J. Gen. Microbiol. **139:**3197–3203.
9. **Guérout-Fleury, A. M., N. Frandsen, and P. Stragier.** 1996. Plasmids for ectopic integration in *Bacillus subtilis*. Gene **180:**57–61.
10. **Hackett, R. H., and P. Setlow.** 1987. Cloning, nucleotide sequencing, and genetic mapping of the gene for small, acid-soluble spore protein γ of *Bacillus subtilis*. J. Bacteriol. **169:**1985–1992.
11. **Harry, E. J., K. Pogliano, and R. Losick.** 1995. Use of immunofluorescence to visualize cell-specific gene expression during sporulation in *Bacillus subtilis*. J. Bacteriol. **177:**3386–3393.
12. **Henner, D. J.** 1990. Inducible expression of regulatory genes in *Bacillus subtilis*. Methods Enzymol. **185:**223–228.
13. **Henriques, A. O., B. W. Beall, and C. P. Moran, Jr.** 1997. CotM of *Bacillus subtilis*, a member of the α-crystallin family of stress proteins, is induced during development and participates in spore outer coat formation. J. Bacteriol. **179:**1887–1897.
14. **Henriques, A. O., B. W. Beall, K. Rowland, and C. P. Moran, Jr.** 1995. Characterization of *cotJ*, a σ^E-controlled operon affecting the polypeptide composition of the coat of *Bacillus subtilis* spores. J. Bacteriol. **177:**3394–3406.
15. **Illing, N., and J. Errington.** 1991. The *spoIIIA* operon of *Bacillus subtilis* defines a new temporal class of mother-cell-specific sporulation genes under the control of the sigma E form of RNA polymerase. Mol. Microbiol. **5:**1927–1940.
16. **Itaya, M., K. Kondo, and T. Tanaka.** 1989. A neomycin resistance gene cassette selectable in a single copy state in the *Bacillus subtilis* chromosome. Nucleic Acids Res. **17:**4410.
17. **Karmazyn-Campelli, C., C. Bonamy, B. Savelli, and P. Stragier.** 1989. Tandem genes encoding σ-factors for consecutive steps of development in *Bacillus subtilis*. Genes Dev. **3:**150–157.
18. **Karow, M. L., and P. J. Piggot.** 1995. Construction of *gusA* transcriptional fusion vectors for *Bacillus subtilis* and their utilization for studies of spore formation. Gene **163:**69–74.
19. **Kellner, E. M., A. Decatur, and C. P. Moran, Jr.** 1996. Two-stage regulation of an anti-sigma factor determines developmental fate during bacterial endospore formation. Mol. Microbiol. **21:**913–924.
20. **Kenney, T. J., and C. P. Moran, Jr.** 1987. Organization and regulation of an operon that encodes a sporulation-essential sigma factor in *Bacillus subtilis*. J. Bacteriol. **169:**3329–3339.
21. **Kirchman, P. A., H. DeGrazia, E. M. Kellner, and C. P. Moran, Jr.** 1993. Forespore-specific disappearance of the sigma-factor antagonist SpoIIAB: implications for its role in determination of cell fate in *Bacillus subtilis*. Mol. Microbiol. **8:**663–671.
22. **Kroos, L., B. Zhang, H. Ichikawa, and Y.-T. N. Yu.** 1999. Control of σ factor activity during *Bacillus subtilis* sporulation. Mol. Microbiol. **31:**1285–1294.
23. **Laskowski, A., M. MacArthur, D. Moss, and J. Thorton.** 1993. PROCHECK: a program to check the stereochemical quality of protein structures. J. Appl. Crystallogr. **26:**283–291.
24. **Londoño-Vallejo, J.-A., C. Fréhel, and P. Stragier.** 1997. *spoIIQ*, a forespore-expressed gene required for engulfment in *Bacillus subtilis*. Mol. Microbiol. **24:**29–39.
25. **Marti-Renom, M., A. Stuart, A. Fiser, R. Sanchez, F. Melo, and A. Sali.** 2000. Comparative protein structure modeling of genes and genomes. Annu. Rev. Biophys. Biomol. Struct. **29:**291–325.
26. **Mason, J. M., R. H. Hackett, and P. Setlow.** 1988. Regulation of transcription of genes coding for small, acid-soluble proteins of *Bacillus subtilis* spores: studies using *lacZ* fusions. J. Bacteriol. **170:**239–244.
27. **Murakami, T., K. Haga, M. Takeuchi, and T. Sato.** 2002. Analysis of the *Bacillus subtilis spoIIIJ* gene and its paralogue gene, *yqjG*. J. Bacteriol. **184:**1998–2004.
28. **Pan, Q., D. A. Garsin, and R. Losick.** 2001. Self-reinforcing activation of a cell-specific transcription factor by proteolysis of an anti-σ factor in *B. subtilis*. Mol. Cell **8:**873–883.
29. **Partridge, S., and J. Errington.** 1993. The importance of morphological events and intercellular interactions in the regulation of prespore-specific gene expression during sporulation in *Bacillus subtilis*. Mol. Microbiol. **8:**945–955.
30. **Piggot, P. J., and J. G. Coote.** 1976. Genetic aspects of bacterial endospore formation. Bacteriol. Rev. **40:**908–962.
31. **Piggot, P. J., and R. Losick.** 2001. Sporulation genes and intercompartmental regulation, p. 483–517. *In* A. L. Sonenshein, J. A. Hoch, and R. Losick (ed.), *Bacillus subtilis* and its closest relatives from genes to cells. ASM Press, Washington, D.C.
32. **Piggot, P. J., J. E. Byland, and M. L. Higgins.** 1994. Morphogenesis and gene expression during sporulation, p. 113–137. *In* P. J. Piggot, C. P. Moran, Jr., and P. Youngman (ed.), Regulation of bacterial differentiation. ASM Press, Washington, D.C.
33. **Pogliano, K., E. Harry, and R. Losick.** 1995. Visualization of the subcellular location of sporulation proteins in *Bacillus subtilis* using immunofluorescence microscopy. Mol. Microbiol. **18:**459–470.
34. **Rather, P. N., and C. P. Moran, Jr.** 1988. Compartment-specific transcription in *Bacillus subtilis*: identification of the promoter *gdh*. J. Bacteriol. **170:**5086–5092.
35. **Rather, P. N., R. Coppolechia, H. deGrazia, and C. P. Moran, Jr.** 1990. Negative regulator of σ^G-controlled gene expression in stationary-phase *Bacillus subtilis*. J. Bacteriol. **172:**709–715.
36. **Rong, S., M. S. Rosenkrantz, and A. L. Sonenshein.** 1986. Transcriptional control of the *Bacillus subtilis spoIID* gene. J. Bacteriol. **165:**771–779.
37. **Rudner, D. Z., and R. Losick.** 2001. Morphological coupling in development: lessons from prokaryotes. Dev. Cell **1:**733–742.
38. **Sali, A., and T. L. Blundell.** 1993. Comparative protein modelling by satisfaction of spatial restraints. J. Mol. Biol. **234:**779–815.
39. **Sánchez, R., and A. Sali.** 1997. Advances in comparative protein-structure modelling. Curr. Opin. Struct. Biol. **7:**206–214.
40. **Schmidt, R., A. L. Decatur, P. N. Rather, C. P. Moran, Jr., and R. Losick.** 1994. *Bacillus subtilis* Lon protease prevents inappropriate transcription of genes under the control of the sporulation transcription factor σ^G. J. Bacteriol. **176:**6528–6537.
41. **Serrano, M., L. Côrte, J. Opdyke, C. P. Moran, Jr., and A. O. Henriques.** 2003. Expression of *spoIIIJ* in the prespore is sufficient for the activation of σ^G and for sporulation in *Bacillus subtilis*. J. Bacteriol. **185:**3905–3917.
42. **Serrano, M., S. Hoevel, C. P. Moran, Jr., A. O. Henriques, and U. Völker.** 2001. Prespore-specific transcription of the *lonB* gene encoding a Lon-like ATP-dependent protease during sporulation in *Bacillus subtilis*. J. Bacteriol. **183:**2032–2040.
43. **Setlow, B., N. Magill, P. Febbroriello, L. Nakhimovsky, D. E. Koppel, and P. Setlow.** 1991. Condensation of the forespore nucleoid early in sporulation of *Bacillus* species. J. Bacteriol. **173:**6270–6278.
44. **Sharp, M. D., and K. Pogliano.** 1999. An in vivo membrane fusion assay implicates SpoIIIE in the final stages of engulfment during *Bacillus subtilis* sporulation. Proc. Natl. Acad. Sci. USA **96:**14553–14558.
45. **Stragier, P.** 1992. Establishment of forespore-specific gene expression during sporulation of *Bacillus subtilis*, p. 297–310. *In* J. A. Cole, F. Mohan, and C. Dow (ed.), Prokaryotic structure and function. Society for General Microbiology, Cambridge, England.
46. **Stragier, P., and R. Losick.** 1996. Molecular genetics of sporulation in *Bacillus subtilis*. Annu. Rev. Genet. **30:**297–341.
47. **Sun, D., R. M. Cabrera-Martinez, and P. Setlow.** 1991. Control of transcription of the *Bacillus subtilis spoIIIG* gene, which codes for the forespore-specific transcription factor σ^G. J. Bacteriol. **173:**2977–2984.
48. **Tjalsma, H., S. Bron, and J. M. van Dijl.** 2003. Complementary impact of paralogous Oxa1-like proteins of *Bacillus subtilis* on posttranslocational stages in protein secretion. J. Biol. Chem. **278:**15622–15632.
49. **Wu, J.-J., M. G. Howard, and P. J. Piggot.** 1989. Regulation of transcription of the *Bacillus subtilis spoIIA* locus. J. Bacteriol. **171:**692–698.
50. **Wu, L. J., and J. Errington.** 1994. *Bacillus subtilis* SpoIIIE protein required for DNA segregation during asymmetric cell division. Science **264:**572–575.
51. **Zilhão, R., M. Serrano, R. Isticato, E. Ricca, and A. O. Henriques.** 2003. Assembly of *Bacillus subtilis* spore coat protein CotB. J. Bacteriol. **186:**1110–1119.
52. **Zuber, P., and R. Losick.** 1987. Role of AbrB in Spo0A- and Spo0B-dependent utilization of a sporulation promoter in *Bacillus subtilis*. J. Bacteriol. **169:**2223–2230.